Unbiased Scattering Function Estimators for Underspread Channels and Extension to Data-Driven Operation

Harold Artés, *Student Member, IEEE*, Gerald Matz, *Member, IEEE*, and Franz Hlawatsch, *Senior Member, IEEE*

***Abstract*—We propose two methods for the estimation of scattering functions of random time-varying channels. In contrast to existing methods, our methods exploit the *underspread property* of these channels to achieve good estimation performance and low computational complexity. The first method uses a dedicated sounding to measure the channel. The second method uses the data signal of an ongoing data transmission as sounding signal and thus allows estimation without dedicated sounding. Both methods are effectively unbiased and can be implemented efficiently using the Zak transform. The performance of our scattering function estimators is studied both analytically by means of variance bounds and experimentally through numerical simulation, and their superiority over existing methods is demonstrated.**

***Index Terms*—Channel sounding, doubly spread targets, fading dispersive channels, mobile radio channels, scattering function estimation, underspread channels, WSSUS channels.**

I. Introduction

THE scattering function (SF) characterizes the second-order statistics of a random, linear time-varying (LTV) channel (or doubly spread random target) that is wide-sense stationary with uncorrelated scatterers (WSSUS) [1]–[3]. Knowledge of the SF is required or at least helpful for a variety of tasks such as optimum receiver design (e.g. [2], [3]), channel estimation [4], [5], synchronization [6], performance evaluation [7], [8], channel capacity analysis [9], and multicarrier system design [10]–[12]. Thus, estimation of the SF is a problem of practical importance.

Several methods for SF estimation are available. A simple and practical SF estimator that is based on the interpretation of the SF as a two-dimensional (2-D) power spectral density is an averaged 2-D periodogram of the measured time-varying transfer function. In [13], a more sophisticated method is proposed that uses a cross-ambiguity function and is based on a statistical input/output relation combined with equalization and smoothing (a preliminary version of this method can be found in [14]). In [15], an SF estimator using a so-called uncertainty product function is presented; this estimator extends the twin processor method previously proposed in [16], [17]. Finally, in [18], estimation of the SF using a 2-D autoregressive (AR) model is discussed.

Except for the averaged periodogram method, these SF estimation methods do not exploit the *underspread* property of most practical mobile radio channels and radar targets [2], [3], [19]–[21]; in fact, Gaarder [13] explains why his method has greater variance in the underspread case than in the overspread case. The averaged periodogram method exploits the underspread property in an implicit manner; however, it is generally biased.

In this paper, we propose two SF estimators that explicitly exploit the underspread property to achieve good estimation performance (in particular, approximate unbiasedness) and low computational complexity [22], [23]. The paper is organized as follows. After reviewing discrete-time LTV channels in Section II and channel sounding in Section III, the first SF estimator is developed in Section IV. In Section V, a statistical analysis and an MMSE-type modification of this estimator are presented. In Section VI, the second estimator is developed and analyzed; this estimator does not use a dedicated sounding and thus allows SF estimation during an ongoing data transmission. Finally, in Section VII, we present simulation results and compare the performance of our estimators with that of existing estimators.

II. Discrete-Time LTV Channels

With a view toward practical implementation, we will consider SF estimation in a discrete-time setting. The discretization of a continuous-time channel is discussed in Appendix A.

A. Characterization of Discrete-Time LTV Channels

The input–output relation of a discrete-time LTV channel $\boldsymbol{H}$ with impulse response $h[n,m]$ is

$$y[n] = \sum_{m=0}^{N_m-1} h[n,m]x[n-m], \quad n \in [0, N-1] \qquad (1)$$

where $N_m - 1$ is the maximum delay of the channel and $[0, N-1]$ is the interval on which the output signal $y[n]$ is considered. We assume $h[n,m]$ to be zero for $n \notin [0, N-1]$ and for $m \notin [0, N_m - 1]$, i.e.,[1] $h[n,m] = 0$ for $(n,m) \notin [0, N-1] \times [0, N_m - 1]$. We also assume that the input signal $x[n]$ has finite length N_x, i.e., $x[n] = 0$ for $n \notin [0, N_x - 1]$, and that $N \geq N_x + N_m - 1$ (see Appendix A for background).

[1]For convenience, we assume one-sided support intervals. Other intervals can easily be accommodated by suitable shifts.

Manuscript received January 10, 2003; revised May 22, 2003. This work was supported by FWF grants P12228-TEC and P15156-N02. The associate editor coordinating the review of this manuscript and approving it for publication was Prof. Tulay Adali.

The authors are with the Institute of Communications and Radio-Frequency Engineering, Vienna University of Technology, A-1040 Wien, Austria (e-mail: hartes@aurora.nt.tuwien.ac.at; gmatz@aurora.nt.tuwien.ac.at; fhlawats@pop.tuwien.ac.at).

Digital Object Identifier 10.1109/TSP.2004.826181

In analogy to the continuous-time case [1], [24], we define the *discrete time-varying transfer function* as the discrete Fourier transform (DFT) of $h[n,m]$ with respect to m:

$$L_{\boldsymbol{H}}[n,k] \triangleq \sum_{m=0}^{N_m-1} h[n,m]e^{\frac{-j2\pi km}{N}}, \quad k \in [0, N-1] \qquad (2)$$

with k denoting discrete frequency. Note that here, the DFT has been zero-padded to length N since it uses $e^{-j2\pi km/N}$ instead of $e^{-j2\pi km/N_m}$. Similarly, the *discrete spreading function* $S_{\boldsymbol{H}}[m,l]$ is defined as the DFT of $h[n,m]$ with respect to n (cf. [1] in the continuous-time case)

$$\begin{aligned} S_{\boldsymbol{H}}[m,l] &\triangleq \sum_{n=0}^{N-1} h[n,m]e^{\frac{-j2\pi ln}{N}} \\ &= \frac{1}{N}\sum_{n=0}^{N-1}\sum_{k=0}^{N-1} L_{\boldsymbol{H}}[n,k]e^{\frac{-j2\pi(ln-mk)}{N}} \\ &\qquad (m,l) \in [0, N-1] \times [0, N-1] \end{aligned}$$

where l is a discrete Doppler shift variable. Hereafter, all signals and their DFTs will be considered as being periodic with period N.

B. WSSUS Channels and Underspread Property

When the discrete-time LTV channel $\boldsymbol{H}$ is random, then so are $h[n,m]$, $S_{\boldsymbol{H}}[m,l]$, and $L_{\boldsymbol{H}}[n,k]$. We now consider the second-order statistics of a random discrete-time LTV channel $\boldsymbol{H}$.

WSSUS Channels and Scattering Function: In analogy to the continuous-time case [1], we will call a random, discrete-time LTV channel $\boldsymbol{H}$ *wide-sense stationary with uncorrelated scatterers* (WSSUS) if $h[n,m]$ is zero-mean and its correlation function is of the form $\mathbb{E}\{h[n,m]h^*[n',m']\} = R_h[n-n',m]\delta[m-m']$. Two equivalent formulations are

$$\mathbb{E}\{L_{\boldsymbol{H}}[n,k]L^*_{\boldsymbol{H}}[n',k']\} = R_L[n-n',k-k'] \qquad (3)$$

with the *(discrete) time-frequency correlation function*

$$R_L[\Delta n, \Delta k] = \sum_{m=0}^{N-1} R_h[\Delta n, m]e^{\frac{-j2\pi m\Delta k}{N}}$$

and

$$\mathbb{E}\{S_{\boldsymbol{H}}[m,l]S^*_{\boldsymbol{H}}[m',l']\} = C[m,l]\delta[m-m']\delta[l-l'] \qquad (4)$$

with the *(discrete) scattering function* (SF)

$$\begin{aligned} C[m,l] &= N\sum_{\Delta n=0}^{N-1} R_h[\Delta n, m]e^{\frac{-j2\pi l\Delta n}{N}} \\ &= \sum_{\Delta n=0}^{N-1}\sum_{\Delta k=0}^{N-1} R_L[\Delta n, \Delta k]e^{\frac{-j2\pi(l\Delta n - m\Delta k)}{N}}. \end{aligned} \qquad (5)$$

According to (3) and (5), $L_{\boldsymbol{H}}[n,k]$ is a *2-D wide-sense stationary* process with correlation function $R_L[\Delta n, \Delta k]$ and power spectral density $C[m,l]$ (the SF). According to (4), scatterers with different delay m and/or Doppler l are *uncorrelated*. The time-frequency correlation function $R_L[\Delta n, \Delta k]$ and the SF $C[m,l]$ are related via a 2-D Fourier transform and, hence, are two equivalent second-order statistics of a WSSUS channel $\boldsymbol{H}$.

Underspread Channels: Motivated by the underspread property in the continuous-time case [2], [3], [19], we call a WSSUS channel *underspread* if its SF is support-limited according to

$$\begin{aligned} C[m,l] = 0 \quad \text{for} \quad & (m,l) \notin [0, N_m-1] \times [0, N_l-1] \\ & \text{with } \frac{N_m N_l}{N} \le 1 \end{aligned} \qquad (6)$$

where $N_l - 1$ is the maximum Doppler shift. According to (4), (6) implies that, with probability one, the spreading function $S_{\boldsymbol{H}}[m,l]$ also satisfies this support constraint. Thus, for an underspread channel, the product of N_m and N_l is bounded by N. Although we have assumed a specific location of the SF support in the (m,l)-plane, the underspread definition in (6) can easily be reformulated for arbitrary locations. Most practical channels and targets satisfy the underspread property.

III. Channel Sounding

Because the SF $C[m,l]$ is the power spectral density of the 2-D process $L_{\boldsymbol{H}}[n,k]$, existing algorithms for 2-D spectral estimation—such as a 2-D periodogram or a 2-D AR estimator [18], [25]—can be used for SF estimation. However, an important difference from conventional spectral estimation is that realizations of the process $L_{\boldsymbol{H}}[n,k]$ can only be obtained by means of a *channel sounding* procedure that generally introduces a systematic error (bias) [26]. Our SF estimation methods are also based on channel sounding but in such a way that the corresponding bias can be compensated. In this section, we review the channel sounding technique we will use. This technique is motivated by a theoretical "impulse-train" sounding scheme that was originally proposed in [27] and [28] in a continuous-time setting.

A. Impulse-Train Channel Sounding

Let $\boldsymbol{H}$ be a discrete-time WSSUS channel with impulse response $h[n,m]$, maximum delay $N_m - 1$, and maximum Doppler shift $N_l - 1$. Let us use as the input (sounding) signal an impulse train with impulse spacing M and total length equal to the block length N (which is chosen as an integer multiple of M):

$$x[n] = \delta_M[n] \triangleq \sum_{r=0}^{\frac{N}{M}-1} \delta[n - rM]. \qquad (7)$$

Hereafter, we assume that the impulse spacing M is matched to N, N_m, and N_l according to

$$N_m \le M \le \frac{N}{N_l}. \qquad (8)$$

Note that this presupposes the underspread property $N_m N_l \leq N$ in (6). The output signal is then obtained from (1) as

$$\begin{aligned} y[n] &= \sum_{m=0}^{M-1} \sum_{r=0}^{\frac{N}{M}-1} h[n,m]\delta[n-m-rM] \\ &= \sum_{r=0}^{\frac{N}{M}-1} h[n, n-rM] \\ &= h\left[n, n-\left\lfloor \frac{n}{M} \right\rfloor M\right] \end{aligned}$$

where the last equation holds since the channel responses to the individual impulses do not overlap (due to $M \geq N_m$). Thus, the output signal $y[n]$ consists of slices of the channel impulse response $h[n,m]$. For fixed m, $h[n,m]$ is subsampled with respect to n by a factor of M. However, $h[n,m]$ is bandlimited with respect to n with bandwidth $N_l - 1$, and, due to our assumption (8), the sampling period M is small enough so that the missing samples can be perfectly reconstructed by means of interpolation. Therefore, using the impulse train sounding scheme, we can indeed obtain the impulse response $h[n,m]$. It should be noted that this is fundamentally based on the underspread property (6).

B. Correlative Channel Sounding

Due to its high crest factor, an impulse-train sounding signal (7) is undesirable in practice. Instead, most practical channel sounders [29]–[31] transmit a general pulse-train sounding signal

$$x[n] = \sum_{r=0}^{\frac{N}{M}-1} g[n-rM] \tag{9}$$

where the transmit pulse $g[n]$ is chosen such that $x[n]$ has a low crest factor. The received signal $y[n]$ is then passed through a receive filter in order to achieve *pulse compression*. Let $f[n]$ denote the impulse response of the receive filter and assume it has finite length N_f. Including measurement noise $w[n]$, i.e.,[2] $y[n] = (\boldsymbol{H}x)[n] + w[n]$, the output of the receive filter is

$$y_f[n] \triangleq (y * f)[n] = ((\boldsymbol{H}x) * f)[n] + w_f[n] \tag{10}$$

where $w_f[n] \triangleq (w * f)[n]$ is the filtered noise.

If the product of maximum Doppler shift N_l and receive filter length N_f satisfies $N_l N_f \ll N$, it can be shown that the LTV channel filter $\boldsymbol{H}$ and the receive filter f approximately commute, i.e., we can consider the receive filter to be moved to the transmitter side [26]. Thus,

$$((\boldsymbol{H}x) * f)[n] \approx (\boldsymbol{H}(x * f))[n] = (\boldsymbol{H}x_v)[n], \quad \text{for } N_l N_f \ll N$$

with the "virtual sounding signal"

$$x_v[n] \triangleq (x * f)[n]. \tag{11}$$

Inserting this approximation into (10), the output of the receive filter becomes

$$y_f[n] \approx y_v[n] \triangleq (\boldsymbol{H}x_v)[n] + w_f[n]. \tag{12}$$

[2]Here, $(\boldsymbol{H}x)[n]$ denotes the output signal of the LTV channel $\boldsymbol{H}$ corresponding to the input signal $x[n]$.

Note that $y_v[n]$ would be obtained if we used the virtual sounding signal $x_v[n]$ as the channel input signal. With (9), the virtual sounding signal is

$$x_v[n] = \sum_{r=0}^{\frac{N}{M}-1} g[n-rM] * f[n] = \sum_{r=0}^{\frac{N}{M}-1} (g * f)[n-rM].$$

In view of Section III-A, $g[n]$ and $f[n]$ must be chosen such that $(g * f)[n] \approx \delta[n]$ (*pulse compression*), i.e., $x_v[n]$ is approximately an impulse train. Thus, we approximate an impulse-train sounding, even though the actual transmit signal $x[n] = \sum_{r=0}^{N/M-1} g[n-rM]$ has a small crest factor. In particular, we can achieve $(g * f)[n] \approx \delta[n]$ by choosing for $g[n]$ a maximum-length pseudonoise sequence and using a *matched* receive filter $f[n] = g^*[-n]$ so that $(g * f)[n]$ becomes the autocorrelation of $g[n]$. We can then obtain a good estimate of slices of the channel impulse response $h[n,m]$ as

$$\hat{h}[rM+m, m] = y_f[rM+m].$$

An estimate of $h[n,m]$ can finally be obtained by interpolating these slices.

IV. Scattering Function Estimator Using Dedicated Sounding Signals

Because the SF is the power spectral density of $L_{\boldsymbol{H}}[n,k]$, it can be estimated (in the case of an underspread channel) by means of the following three-step procedure (e.g. [30]).

1) A realization of $h[n,m]$ is measured using correlative channel sounding, as discussed above.
2) The corresponding realization of $L_{\boldsymbol{H}}[n,k]$ is calculated according to (2).
3) A 2-D spectral estimator is applied to $L_{\boldsymbol{H}}[n,k]$.

The performance of such an approach is limited by the channel sounding. Specifically, application of correlative channel sounding to *fast* time-varying channels (i.e., channels with large N_l) requires a small receive filter length N_f to keep the "commutation error" $y_f[n] - y_v[n]$ (cf. (12)) small. However, a small N_f results in poor pulse compression, which also yields systematic sounding errors [26].

We will now introduce a novel SF estimator that does not employ the straightforward three-step methodology described above. While our estimator also uses correlative channel sounding, it is formulated in such a way that systematic sounding errors do not result in systematic SF estimation errors. Indeed, it is effectively *unbiased* even for nonideal virtual sounding signals with poor pulse compression properties, thereby admitting a wide range of sounding signals and, thus, also supporting fast time-varying channels.

A. Initial Formulation of the SF Estimator

The proposed SF estimator can be motivated as follows [22], [23]. Let the (discrete) ambiguity function $A_x[m,l]$ be defined as [32]

$$A_x[m,l] \triangleq \sum_{n=0}^{N-1} x[n]x^*[n-m]e^{\frac{-j2\pi ln}{N}}$$

where, as before, the length-N signal $x[n]$ is assumed to be periodically repeated with period N. For a (generally nonstationary) random process $x[n]$, we denote by $\bar{A}_x[m,l] \triangleq \mathbb{E}\{A_x[m,l]\}$ the expectation of $A_x[m,l]$. We now consider correlative channel sounding, as described in the previous section. It can be shown (cf. [13] for the continuous-time case) that the relation $y_v[n] = (\boldsymbol{H}x_v)[n] + w_f[n]$ in (12), where $x_v[n]$ is deterministic and $w_f[n]$ is random and statistically independent of $\boldsymbol{H}$, entails the "statistical input-output relation"

$$\bar{A}_{y_v}[m,l] = R_L[m,l]A_{x_v}[m,l] + \bar{A}_{w_f}[m,l]. \tag{13}$$

Assuming approximate commutation of channel and receive filter so that $y_f[n] \approx y_v[n]$ according to (12), we have $\bar{A}_{y_f}[m,l] \approx \bar{A}_{y_v}[m,l]$. Inserting this into (13), it follows that the time-frequency correlation function $R_L[\Delta n, \Delta k]$ can approximately be written as $R_L[\Delta n, \Delta k] \approx [\bar{A}_{y_f}[\Delta n, \Delta k] - \bar{A}_{w_f}[\Delta n, \Delta k]]/A_{x_v}[\Delta n, \Delta k]$, provided that $A_{x_v}[\Delta n, \Delta k] \neq 0$. This suggests that we define an estimate of $R_L[\Delta n, \Delta k]$ as

$$\hat{R}_L[\Delta n, \Delta k] \triangleq \frac{\hat{A}_{y_f}[\Delta n, \Delta k] - \bar{A}_{w_f}[\Delta n, \Delta k]}{A_{x_v}[\Delta n, \Delta k]}. \tag{14}$$

Here

$$\hat{A}_{y_f}[m,l] \triangleq \frac{1}{L}\sum_{i=0}^{L-1} A_{y_f^{(i)}}[m,l] \tag{15}$$

is an estimator of $\bar{A}_{y_f}[m,l]$ that is calculated from L different channel output signals $y_f^{(i)}[n]$. These output signals are obtained by sounding the channel L times, as described in Section III-B. (Due to the WSSUS assumption, the channel's statistics do not change over time, and hence, repeated sounding is not a problem in general.) Furthermore, $\bar{A}_{w_f}[m,l]$ is assumed to be known. Hereafter, we assume that the channel noise $w[n]$ is white with known variance $\mathrm{var}\{w[n]\} = N_0$. It is then easily shown that

$$\bar{A}_{w_f}[m,l] = NN_0 r_f[m]\delta[l], \quad \text{with } r_f[m] \triangleq \sum_{n=0}^{N-1} f[n]f^*[n-m]. \tag{16}$$

Finally, an estimator of the SF $C[m,l]$ can easily be obtained from $\hat{R}_L[\Delta n, \Delta k]$ in (14) by invoking the second Fourier transform relation in (5).

A problem with the estimator (14) is that the division by $A_{x_v}[\Delta n, \Delta k]$ will amplify errors in the estimate $\hat{A}_{y_f}[\Delta n, \Delta k]$ if $|A_{x_v}[\Delta n, \Delta k]|$ is small for some $(\Delta n, \Delta k)$. Unfortunately, from the relation $|A_x[0,0]|^2 = (1/N)\sum_{m=0}^{N-1}\sum_{l=0}^{N-1}|A_x[m,l]|^2$ (a similar relation in the continuous-time case is known as the *radar uncertainty principle* [33], [34]), we can deduce that there does not exist any signal $x_v[n]$ for which $|A_{x_v}[m,l]|$ is approximately constant for all (m,l).

B. "Subsampled" SF Estimator

This problem can, however, be fixed due to the channel's underspread property. We recall from (6) that $C[m,l]$ is confined to the support rectangle $[0, N_m - 1] \times [0, N_l - 1]$ with $N_m N_l/N \leq 1$. Thus, $C[m,l]$ can be reconstructed from a *subsampled* version of the time-frequency correlation function $R_L[\Delta n, \Delta k]$. Let us consider the subsampling defined by $\Delta n = rM$, $\Delta k = sN/M$ with $r, s \in \mathbb{Z}$. With $R_L[\Delta n, \Delta k] = (1/N^2)\sum_{m=0}^{N-1}\sum_{l=0}^{N-1} C[m,l]e^{j2\pi(l\Delta n - m\Delta k)/N}$ (cf. (5)), one can show the relation

$$\sum_{r=0}^{\frac{N}{M}-1}\sum_{s=0}^{M-1} R_L\left[rM, s\frac{N}{M}\right] e^{\frac{-j2\pi(rMl - s\frac{N}{M}m)}{N}} = \frac{1}{N}\sum_{r=0}^{\frac{N}{M}-1}\sum_{s=0}^{M-1} C\left[m - rM, l - s\frac{N}{M}\right]. \tag{17}$$

Due to (8), the individual terms $C[m - rM, l - sN/M]$ in (17) do not overlap. Hence, $C[m,l]$ can be fully reconstructed from $R_L[rM, sN/M]$.

We are thus led to consider the following subsampled version of our estimator (14):

$$\hat{R}_L\left[rM, s\frac{N}{M}\right] = \frac{\hat{A}_{y_f}\left[rM, s\frac{N}{M}\right] - NN_0 r_f[rM]\delta[s]}{A_{x_v}\left[rM, s\frac{N}{M}\right]} \tag{18}$$

with $r = 0, 1, \cdots, N/M - 1$, $s = 0, 1, \cdots, M - 1$. [Note that we have incorporated (16).] Evidently, here, we just have to find a virtual sounding signal $x_v[n]$ for which $|A_{x_v}[m,l]|$ is sufficiently bounded away from zero for $m = rM$ and $l = sN/M$. From $\hat{R}_L[rM, sN/M]$, an estimate of the SF can be obtained by invoking (17) on the fundamental support rectangle, which results in the following 2-D DFT:

$$\hat{C}[m,l] \triangleq N\sum_{r=0}^{\frac{N}{M}-1}\sum_{s=0}^{M-1} \hat{R}_L\left[rM, s\frac{N}{M}\right] e^{-j2\pi\left(\frac{lr}{N/M} - \frac{ms}{M}\right)} \quad (m,l) \in [0, N_m - 1] \times [0, N_l - 1]. \tag{19}$$

(Note that $C[m,l]$ is known to be zero for $(m,l) \notin [0, N_m - 1] \times [0, N_l - 1]$.) If the length of the receive filter is smaller than or equal to the pulse spacing, i.e., $N_f \leq M$, we have $r_f[rM] = E_f\delta[r]$ with $E_f = r_f[0]$. Here, the estimator (19) simplifies to

$$\hat{C}[m,l] = N\sum_{r=0}^{\frac{N}{M}-1}\sum_{s=0}^{M-1} \frac{\hat{A}_{y_f}\left[rM, s\frac{N}{M}\right]}{A_{x_v}\left[rM, s\frac{N}{M}\right]} e^{-j2\pi\left(\frac{lr}{N/M} - \frac{ms}{M}\right)} - \gamma \tag{20}$$

where $\gamma = N^2 N_0 E_f / E_{x_v}$, with $E_{x_v} = \sum_{n=0}^{N-1}|x_v[n]|^2 = A_{x_v}[0,0]$.

A bias/variance analysis of our SF estimator will be provided in Section V-A; in particular, it will be shown that the estimator is effectively unbiased even for a nonideal virtual sounding signal $x_v[n]$.

Ideal Virtual Sounding Signal; Relation to Averaged Periodogram Estimator: If the virtual sounding signal is an ideal impulse train, i.e., $x_v[n] = \delta_M[n] = \sum_{i=0}^{N/M-1}\delta[n - iM]$, the ambiguity function of $x_v[n]$ is the "bed of spikes" $A_{\delta_M}[m,l] = (N/M)\sum_{r=0}^{N/M-1}\sum_{s=0}^{M-1}\delta[m - rM]\delta[l - sN/M]$. In particular, the *subsampled* ambiguity function is *constant*:

$$A_{\delta_M}\left[rM, s\frac{N}{M}\right] \equiv \frac{N}{M}. \tag{21}$$

Thus, for an ideal impulse train sounding signal, the "equalization" corresponding to the division by $A_{x_v}[rM, sN/M]$ in (20)

reduces to a mere scaling operation, and our SF estimator becomes

$$\hat{C}[m,l]\Big|_{x_v[n]=\delta_M[n]} = M\sum_{r=0}^{\frac{N}{M}-1}\sum_{s=0}^{M-1}\hat{A}_{y_f}\left[rM, s\frac{N}{M}\right] \times e^{-j2\pi\left(\frac{lr}{N}-\frac{ms}{M}\right)} - \gamma. \quad (22)$$

Whereas $|A_x[rM, sN/M]| \le A_x[0,0]$ for all $x[n]$, the impulse train $\delta_M[n]$ satisfies $A_{\delta_M}[rM, sN/M] = A_{\delta_M}[0,0]$. Thus, $A_x[rM, sN/M]$ is maximized by $x[n] = \delta_M[n]$. In Section V-A, we will see that this is favorable for a low estimator variance.

Consider now the *averaged periodogram SF estimator*, which is defined as

$$\begin{aligned}\hat{C}_{\mathrm{per}}[m,l] &\triangleq \frac{1}{L}\sum_{i=0}^{L-1}\left|\hat{S}_{\boldsymbol{H}}^{(i)}[m,l]\right|^2 \\ &= \frac{1}{L}\sum_{i=0}^{L-1}\left|\frac{1}{N}\sum_{n=0}^{N-1}\sum_{k=0}^{N-1}\hat{L}_{\boldsymbol{H}}^{(i)}[n,k]e^{\frac{-j2\pi(ln-mk)}{N}}\right|^2 \quad (23)\end{aligned}$$

where $\hat{S}_{\boldsymbol{H}}^{(i)}[m,l]$ and $\hat{L}_{\boldsymbol{H}}^{(i)}[n,k]$ are, respectively, the spreading function and time-varying transfer function of the channel measurement obtained from the ith sounding. (Recall that $C[m,l]$ is the power spectral density of $L_{\boldsymbol{H}}[n,k]$; thus, $|(1/N)\sum_{n=0}^{N-1}\sum_{k=0}^{N-1}\hat{L}_{\boldsymbol{H}}^{(i)}[n,k]e^{-j2\pi(ln-mk)/N}|^2$ is indeed a periodogram [25], [35].) It can then be shown that up to the noise bias correction γ, the SF estimator for $x_v[n] = \delta_M[n]$ in (22) is equal to the averaged periodogram SF estimator $\hat{C}_{\mathrm{per}}[m,l]$, i.e.,

$$\hat{C}[m,l]\Big|_{x_v[n]=\delta_M[n]} = \hat{C}_{\mathrm{per}}[m,l] - \gamma. \quad (24)$$

Conversely, we can say that in the general case, our SF estimator in (20) is an extension of the averaged periodogram SF estimator which adds i) an "equalization" that allows to compensate the detrimental effect of a nonideal sounding signal and ii) a noise bias correction. As we will see in Section V-A, these measures cause our estimator to be effectively unbiased.

C. Efficient Implementation Using the Zak Transform

An efficient implementation of the SF estimator in (19) is based on the *discrete Zak transform*, which is defined as [36]

$$Z_y[m,l] \triangleq \sum_{r=0}^{\frac{N}{M}-1} y[m+rM]e^{-j2\pi\frac{lr}{N/M}}.$$

Using the relations $y[m] = (M/N)\sum_{l=0}^{N/M-1} Z_y[m,l]$ and $Z_y[m+rM,l] = Z_y[m,l]e^{j2\pi rl/(N/M)}$ [36], it can be shown that the subsampled ambiguity function can be expressed in terms of $Z_y[m,l]$ as

$$A_y\left[rM, s\frac{N}{M}\right] = \frac{M}{N}\sum_{m=0}^{M-1}\sum_{l=0}^{N/M-1}|Z_y[m,l]|^2 e^{j2\pi\left(\frac{lr}{N/M}-\frac{ms}{M}\right)}.$$

Therefore, we can write the subsampled version of (15) as

$$\hat{A}_{y_f}\left[rM, s\frac{N}{M}\right] = \frac{M}{N}\sum_{m=0}^{M-1}\sum_{l=0}^{\frac{N}{M}-1} z[m,l]e^{j2\pi\left(\frac{lr}{N/M}-\frac{ms}{M}\right)}$$
$$\text{with } z[m,l] \triangleq \frac{1}{L}\sum_{i=0}^{L-1}\left|Z_{y_f^{(i)}}[m,l]\right|^2. \quad (25)$$

Inserting this expression into (20), we obtain an efficient implementation of the SF estimator. Indeed, a single Zak transform can be computed efficiently using M N/M-point fast Fourier transforms (FFTs), which corresponds to a computational complexity of $\mathcal{O}(M\cdot(N/M)\log(N/M)) = \mathcal{O}(N\log(N/M))$. Taking all other operations into account, the overall computational complexity of the estimator $\hat{C}[m,l]$ in (20) is obtained as $\mathcal{O}(LN\log(N/M))$.

We finally note that

$$\begin{aligned}\left|Z_{y_f^{(i)}}[m,l]\right|^2 &= \left|\hat{S}_{\boldsymbol{H}}^{(i)}[m,l]\right|^2 \\ &= \left|\sum_{r=0}^{\frac{N}{M}-1}\hat{h}^{(i)}[m+rM,m]e^{-j2\pi\frac{lr}{N/M}}\right|^2 \\ &\qquad (m,l)\in[0,N_m-1]\times[0,N_l-1]\end{aligned}$$

provided that (8) is satisfied. This relation, combined with (25), can be used to show (24).

D. "Subsubsampled" SF Estimator

Further computational savings can be achieved if the channel is strongly underspread, i.e., if $N_mN_l \ll N$. Let us assume that N is an integer multiple of both N_m and N_l, i.e., $N/N_m \in \mathbb{N}$ and $N/N_l \in \mathbb{N}$. Then, the time-frequency correlation function $R_L[\Delta n, \Delta k]$ need only be calculated on the lattice (rN/N_l, sN/N_m) that is sparser than the lattice (rM,sN/M) used previously. The corresponding SF estimator is given by

$$\hat{C}[m,l] = N_mN_l\sum_{r=0}^{N_l-1}\sum_{s=0}^{N_m-1}\hat{R}_L\left[r\frac{N}{N_l}, s\frac{N}{N_m}\right]e^{-j2\pi\left(\frac{lr}{N_l}-\frac{ms}{N_m}\right)}$$
$$(m,l)\in[0,N_m-1]\times[0,N_l-1]$$

with

$$\hat{R}_L\left[r\frac{N}{N_l}, s\frac{N}{N_m}\right] = \frac{\hat{A}_{y_f}\left[r\frac{N}{N_l}, s\frac{N}{N_m}\right] - NN_0r_f\left[r\frac{N}{N_l}\right]\delta[s]}{A_{x_v}\left[r\frac{N}{N_l}, s\frac{N}{N_m}\right]}.$$

The "subsubsampled" ambiguity function estimate $\hat{A}_{y_f}[rN/N_l, sN/N_m]$ can again be calculated efficiently as

$$\hat{A}_{y_f}\left[r\frac{N}{N_l}, s\frac{N}{N_m}\right] = \frac{1}{N_l}\sum_{m=0}^{N_m-1}\sum_{l=0}^{N_l-1}\tilde{z}[m,l]e^{j2\pi\left(\frac{lr}{N_l}-\frac{ms}{N_m}\right)}$$
$$\text{where } \tilde{z}[m,l] \triangleq \frac{1}{L}\sum_{i=0}^{L-1}\left|\widetilde{Z}_{y_f^{(i)}}[m,l]\right|^2$$

with the Zak transform $\widetilde{Z}_y[m,l] \triangleq \sum_{r=0}^{N_l-1} y[m + rN/N_l]e^{-j2\pi lr/N_l}$. The overall computational complexity of this "subsubsampled" SF estimator $\hat{C}[m,l]$ is $\mathcal{O}(LNN_m\log(N_l)/M)$.

V. Bias/Variance Analysis and MMSE-Type Equalization

We next analyze the bias and variance of the proposed SF estimator $\hat{C}[m,l]$ in (19). We also present a modified estimator that allows us to reduce the variance at the expense of a nonzero bias.

A. Bias/Variance Analysis

For bias/variance analysis, we neglect the commutation error caused by imperfect commutation of channel and receive filter so that $y_f[n]$ can be replaced by $y_v[n]$. However, we do not assume perfect pulse compression, i.e., $x_v[n] \neq \delta_M[n]$ in general.

Bias: With (13) and $\mathbb{E}\{\hat{A}_{y_f}[m,l]\} = \bar{A}_{y_f}[m,l] = \bar{A}_{y_v}[m,l]$, it follows that *the estimator* $\hat{C}[m,l]$ *in* (19) *is unbiased*, i.e., $\mathbb{E}\{\hat{C}[m,l]\} \equiv C[m,l]$. This is due to the noise bias correction (subtraction of $\bar{A}_{w_f}[rM, sN/M] = NN_0 r_f[rM]\delta[s]$) and the "equalization" (division by $A_{x_v}[rM, sN/M]$) in (18).

Variance: Next, we consider the average variance of $\hat{C}[m,l]$

$$V \triangleq \frac{1}{N} \sum_{m=0}^{M-1} \sum_{l=0}^{\frac{N}{M}-1} \operatorname{var}\left\{\hat{C}[m,l]\right\}. \tag{26}$$

We assume that $h[n,m]$ and $w[n]$ are circularly symmetric complex Gaussian processes and are statistically independent. We also assume that all channel measurements are statistically independent, which requires that two consecutive channel soundings are spaced farther apart in time than the channel's coherence time [2]. Even with these assumptions, a reasonably simple closed-form expression of V does not exist. However, it is shown in Appendix B that V is upper bounded as

$$V \leq \frac{\beta N}{L} \sum_{r=0}^{\frac{N}{M}-1} \sum_{s=0}^{M-1} \frac{1}{\left|A_{x_v}\left[rM, s\frac{N}{M}\right]\right|^2}. \tag{27}$$

Here

$$\beta \triangleq NE_{x_v}^2 R_L^2[0,0] + 2NN_0 E_{x_v} R_L[0,0] \left|F[k]\right|_{\max}^2 + NN_0^2 \left\| |F[k]|^2 \right\|^2$$

with $E_{x_v} = \sum_{n=0}^{N-1} |x_v[n]|^2 = A_{x_v}[0,0]$ and the path loss [2] $R_L[0,0] = (1/N^2) \sum_{m=0}^{M-1} \sum_{l=0}^{N/M-1} C[m,l]$. The important message of (27) is that the variance must be expected to be high if $|A_{x_v}[rM, sN/M]|$ contains small values, and it will be lower for more averaging (i.e., a larger number of soundings, L).

For perfect pulse compression, i.e., $x_v[n] = K\delta_M[n]$ (with K some constant factor), we have $A_{x_v}[rM, sN/M] \equiv |K|^2 N/M = E_{x_v}$ according to (21), and thus, the upper bound (27) becomes

$$V|_{x_v[n]=K\delta_M[n]} \leq \frac{\beta M^2}{L|K|^4} = \frac{\beta}{L} \frac{N^2}{E_{x_v}^2}.$$

There is $|A_{x_v}[rM, sN/M]|^2 \leq E_{x_v}^2$ for any signal $x_v[n]$. Thus, for fixed E_{x_v}, the variance bound in (27) is minimized by $x_v[n] = K\delta_M[n]$, in which case, $|A_{x_v}[rM, sN/M]| \equiv E_{x_v}$.

We conclude that while our estimator is unbiased for any virtual sounding signal, the variance bound will be smallest for an ideal virtual sounding signal (perfect pulse compression). We can thus expect that a nonideal virtual sounding signal leads to a larger estimation variance. This is not a real problem, however, since the variance can always be decreased by more averaging (i.e., a larger L). This will be verified experimentally in Section VII. In contrast, a nonzero bias cannot be decreased by averaging.

Finally, we note that the variance can be reduced by a smoothing of $\hat{C}[m,l]$. Such a smoothing is similar to certain smoothing methods used in spectral estimation [25], [35]. Unfortunately, smoothing results in a nonzero bias that will be small only if the SF is itself smooth. We will next describe an alternative method for variance reduction.

B. MMSE-Type Equalization

Together with the noise bias correction, the division by $A_{x_v}[rM, sN/M]$ in (18) causes our estimator to be effectively unbiased for any $x_v[n]$, and thus, this division can be viewed as a "zero-forcing equalization." However, as shown above, this equalization must be expected to result in a larger variance if some values $A_{x_v}[rM, sN/M]$ are small, i.e., if $x_v[n]$ has poor pulse compression properties. If the number of soundings L is limited (e.g., because the channel statistics are not exactly constant with respect to time), variance reduction by averaging is limited as well. It may then be wise to replace the denominator in (18) $A_{x_v}[rM, sN/M]$ with some other "equalization function" $D[r,s]$ that leads to a variance reduction at the expense of a nonzero bias. Thus, we consider

$$\hat{R}_{L,\mathrm{b}}\left[rM, s\frac{N}{M}\right] \triangleq \frac{\hat{A}_{y_f}\left[rM, s\frac{N}{M}\right] - NN_0 r_f[rM]\delta[s]}{D[r,s]}$$

from which a biased SF estimator $\hat{C}_{\mathrm{b}}[m,l]$ is obtained via a 2-D DFT as in (19).

Adopting a minimum mean-square error (MMSE) approach, we would like to choose the $D[r,s]$ that minimizes the average mean-square error (MSE)

$$\mathrm{MSE} \triangleq \frac{1}{N} \sum_{m=0}^{M-1} \sum_{l=0}^{\frac{N}{M}-1} \mathbb{E}\left\{\left|\hat{C}_{\mathrm{b}}[m,l] - C[m,l]\right|^2\right\}.$$

Unfortunately, this $D[r,s]$ depends on the SF that is unknown. We will therefore calculate the $D[r,s]$ that minimizes a simple upper bound on the MSE. We have $\mathrm{MSE} = B + V$ with the average (squared) bias $B \triangleq (1/N) \sum_{m=0}^{M-1} \sum_{l=0}^{N/M-1} |\mathbb{E}\{\hat{C}_{\mathrm{b}}[m,l]\} - C[m,l]|^2$ and the average variance V defined in (26). It can be shown that

$$B \leq N^2 R_L^2[0,0] \sum_{r=0}^{\frac{N}{M}-1} \sum_{s=0}^{M-1} \left|1 - \frac{A_{x_v}\left[rM, s\frac{N}{M}\right]}{D[r,s]}\right|^2.$$

Furthermore, a bound on V is given by (27) with $A_{x_v}[rM, sN/M]$ replaced by $D[r,s]$. Thus, we obtain

$$\mathrm{MSE} \leq \sum_{r=0}^{\frac{N}{M}-1} \sum_{s=0}^{M-1} \left[\frac{\beta N}{L|D[r,s]|^2} + N^2 R_L^2[0,0] \left|1 - \frac{A_{x_v}\left[rM, s\frac{N}{M}\right]}{D[r,s]}\right|^2\right].$$

Since all terms of this sum are non-negative, each term can be minimized separately. The result is

$$D[r,s] = \frac{\left|A_{x_v}\left[rM, s\frac{N}{M}\right]\right|^2 + \frac{\beta}{NLR_L^2[0,0]}}{A^*_{x_v}\left[rM, s\frac{N}{M}\right]} = A_{x_v}\left[rM, s\frac{N}{M}\right] + \frac{\beta}{NLR_L^2[0,0]A^*_{x_v}\left[rM, s\frac{N}{M}\right]}.$$

Compared to the unbiased case where $D[r,s] = A_{x_v}[rM, sN/M]$, the additional term $\beta/(NLR_L^2[0,0]A^*_{x_v}[rM, sN/M])$ stabilizes the estimator in the case of a poor virtual sounding signal $x_v[n]$, where $A_{x_v}[rM, sN/M]$ is partly small. This additional term becomes smaller for a larger number of soundings L and for weaker noise (smaller N_0); however, it does not vanish for $N_0 = 0$. Note that $D[r,s]$ depends on the path loss $R_L[0,0] = (1/N^2)\sum_{m=0}^{M-1}\sum_{l=0}^{N/M-1} C[m,l]$, which is unknown *a priori* but can be estimated quite easily.

VI. Data-Driven Scattering Function Estimation

In this section, we extend our SF estimator to online operation during data transmission [23]. Here, a segment of the data signal actually transmitted is used as the sounding signal $x[n]$. This signal is assumed to be known at the receiver (i.e., it is assumed that the corresponding data symbols have been detected). The advantage of such a *data-driven* SF estimation is that the SF can be continually estimated (monitored) during an ongoing data transmission, with no need for separate sounding phases. However, a difficulty is that typical data signals do not lead to appropriate virtual sounding signals that are similar to a periodic impulse train. To overcome this problem, we propose a "matched filterbank" (see Fig. 1) that performs the twofold task of pulse compression and periodization.

A. Data-Driven Channel Sounding

In the following, we model the data signal $x[n]$ as a stationary random process with autocorrelation $R_x[m] = \mathbb{E}\{x[n]x^*[n-m]\}$ of correlation width N_{R_x} (i.e., $R_x[m]$ is effectively zero for $|m| > N_{R_x}$).

Matched Receive Filters: Consider the N/M receive filters

$$f_r[n] = \mathrm{rect}_{N_f}[-n]x^*[-(n-rM)], \quad r = 0, 1, \cdots, \frac{N}{M} - 1$$

where $\mathrm{rect}_{N_f}[n]$ is 1 on the interval $[0,\ N_f - 1]$ and 0 elsewhere. Thus, $f_r[n]$ is matched to the segment of the data signal $x[n]$ located in the interval $[rM, rM + N_f - 1]$. Again, we will consider $f_r[n]$ to be periodically continued with period N. The filter length N_f is chosen short enough so that the commutation error (incurred by commuting the receive filters f_r and the channel $\boldsymbol{H}$; see Section III-B) is negligible.

The output signals of the various receive filters are given by [cf. (12) and Fig. 1]

$$y_{f_r}[n] = (y * f_r)[n] \approx \left(\boldsymbol{H}x_v^{(r)}\right)[n] + w_{f_r}[n] \qquad (28)$$

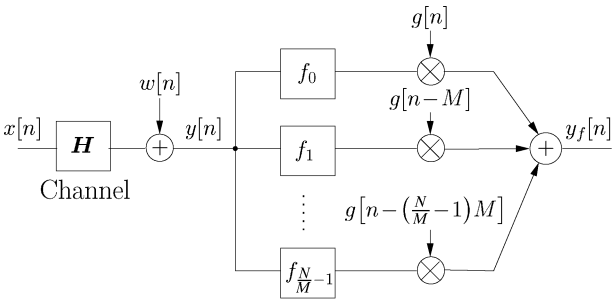

Fig. 1. Matched receive filterbank for data-driven sounding.

with the filtered noise $w_{f_r}[n] = (w * f_r)[n]$ and the virtual sounding signal [cf. (11)]

$$x_v^{(r)}[n] = (x * f_r)[n] = \sum_{n'=n}^{n+N_f-1} x[n']x^*[n' - (n - rM)] = N_f\hat{R}_x^{(r)}[n - rM].$$

Here, $\hat{R}_x^{(r)}[m] \triangleq (1/N_f)\sum_{n=rM+m}^{rM+m+N_f-1} x[n]x^*[n-m]$ is an unbiased estimate of the autocorrelation $R_x[m]$. If N_{R_x} is small so that $R_x[m]$ is narrow and if N_f is sufficiently large so that $\hat{R}_x^{(r)}[m] \approx R_x[m]$, then $x_v^{(r)}[n]$ will be a reasonable approximation to an impulse at $n = rM$.

The choice of the receive filter length N_f is governed by two conflicting requirements: For small commutation errors, N_f should be small, whereas for $\hat{R}_x^{(r)}[m] \approx R_x[m]$, N_f should be large. However, we will see in Section VI-C that for data-driven SF estimation, sounding errors resulting from a small N_f can be compensated by more averaging.

Noise-Suppression Windowing: We will next explain the windows $g[n - rM]$ in Fig. 1. Consider the output of the rth receive filter $y_{f_r}[n]$ in (28). The channel is causal and has maximum delay $N_m - 1$. Let us assume that $\hat{R}_x^{(r)}[m] \approx R_x[m]$, and recall that $R_x[m] \approx 0$ for $|m| > N_{R_x}$. It follows that the term $\boldsymbol{H}\{x_v^{(r)}[n]\} = N_f\boldsymbol{H}\{\hat{R}_x^{(r)}[n - rM]\} \approx N_f\boldsymbol{H}\{R_x[n - rM]\}$ in (28) is approximately zero outside the interval $[-N_{R_x} + rM,\ N_{R_x} + rM + N_m - 1]$. Hence, outside this interval, $y_{f_r}[n]$ is essentially noise. We can suppress this noise and thus reduce sounding errors by windowing $y_{f_r}[n]$ according to (see Fig. 1)

$$y_{f_r}^{(g)}[n] \triangleq y_{f_r}[n]g[n - rM]$$

where $g[n]$ is a window whose effective support contains $[-N_{R_x},\ N_{R_x} + N_m - 1]$.

While a more general window $g[n]$ will be allowed further below, here, we assume a rectangular window $g[n] = \mathrm{rect}_M[n + N_{R_x}]$ for simplicity, i.e., $g[n]$ is 1 on $[-N_{R_x},\ -N_{R_x} + M - 1]$ and 0 elsewhere (we assume that $2N_{R_x} + N_m < M$ so that the interval $[-N_{R_x},\ N_{R_x} + N_m - 1]$ is contained in the interval $[-N_{R_x},\ -N_{R_x} + M - 1]$).

Matched Receive Filterbank: Under the assumptions stated, $x_v^{(r)}[n]$ approximates an impulse at $n = rM$. To obtain a virtual sounding signal that approximates a periodic impulse train, it thus suffices to add the outputs of all matched receive filters

(see Fig. 1). The output signal of the resulting *matched receive filterbank* is

$$y_f[n] = \sum_{r=0}^{\frac{N}{M}-1} y_{f_r}^{(g)}[n] = \sum_{r=0}^{\frac{N}{M}-1} (y * f_r)[n] g[n - rM] \quad (29)$$
$$\approx \sum_{r=0}^{\frac{N}{M}-1} \left(\boldsymbol{H} x_v^{(r)}\right)[n] g[n - rM] + w_f[n]$$

with the filtered and windowed noise

$$w_f[n] = \sum_{r=0}^{\frac{N}{M}-1} (w * f_r)[n] g[n - rM]$$
$$= \sum_{r=0}^{\frac{N}{M}-1} \sum_{m=0}^{N-1} w[n-m] f_r[m] g[n - rM].$$

Because the windows $g[n - rM]$ approximately pass the "signal" components $(\boldsymbol{H}x_v^{(r)})[n]$, we obtain

$$y_f[n] \approx \sum_{r=0}^{\frac{N}{M}-1} \left(\boldsymbol{H} x_v^{(r)}\right)[n] + w_f[n] = (\boldsymbol{H} x_v)[n] + w_f[n]$$

with the virtual sounding signal

$$x_v[n] = \sum_{r=0}^{\frac{N}{M}-1} x_v^{(r)}[n] = N_f \sum_{r=0}^{\frac{N}{M}-1} \hat{R}_x^{(r)}[n - rM].$$

If the assumption $\hat{R}_x^{(r)}[m] \approx R_x[m]$ is not well satisfied, sounding errors will occur. Moreover, the noise-suppression windowing may truncate parts of $(\boldsymbol{H}x_v^{(r)})[n] = N_f \boldsymbol{H}\{\hat{R}_x^{(r)}[n - rM]\}$ and thus cause additional sounding errors. However, in Section VI-B, we will present a statistical input–output relation showing that these errors cancel on average.

Noise Power: For later use, we calculate the mean power of $w_f[n]$. We assume that $f_r[n]$ and $f_{r'}[n]$ do not overlap for $r \neq r'$ (i.e., $N_f \leq M$) and that the energies $E_{f_r} \triangleq \sum_{n=0}^{N-1} |f_r[n]|^2$ of all $f_r[n]$ are approximately equal, i.e., $E_{f_r} \approx E_f$ for all r. We can then show that

$$\mathbb{E}\left\{|w_f[n]|^2\right\} = N_0 \sum_{r=0}^{\frac{N}{M}-1} E_{f_r} |g[n - rM]|^2 \approx N_0 E_f$$

where in the last step, we used the fact that $\sum_{r=0}^{N/M-1} |g[n - rM]|^2 = 1$ on the fundamental time interval $[0, N-1]$. Without noise-suppression windowing (i.e., for $g[n] \equiv 1$), we would obtain a noise power of approximately $N_0(N/M)E_f$. Thus, the windowing reduces the noise power by a factor of about N/M.

B. Data-Driven Scattering Function Estimator

The proposed data-driven SF estimator is based on the data-driven channel sounding described above. It is motivated by a "statistical input/output relation" that is analogous to (13). As before, we neglect the commutation error caused by imperfect commutation of channel H and receive filters f_r. We assume that the data signal $x[n]$, the channel impulse response $h[n, m]$, and the white noise $w[n]$ are circularly symmetric Gaussian and statistically independent and that $R_x[m] = 0$ for $|m| > N_{R_x}$ with $N_{R_x} \leq \lfloor M/2 \rfloor$ and $N_f + N_{R_x} \leq M$. The noise suppression window $g[n]$ is assumed to satisfy $\sum_{r=0}^{N/M-1} |g[n - rM]|^2 \equiv c$ (constant) and $g[n] = 1$ for $n \in [-N_{R_x}, N_{R_x} + N_m - 1]$. It is then shown in Appendix C that the subsampled expected ambiguity function of the matched receive filterbank output $y_f[n]$ in (29) is

$$\bar{A}_{y_f}\left[rM, s\frac{N}{M}\right] = \frac{N_f^2 N}{M} A_{R_x}\left[0, s\frac{N}{M}\right] \times R_L\left[rM, s\frac{N}{M}\right] + \alpha\delta[r]\delta[s] \quad (30)$$

with

$$\alpha \triangleq cN\left[R_L[0,0] \sum_{m=-N_f+1}^{N_f-1} |R_x[m]|^2 (N_f - m) + N_0 N_f R_x[0]\right]. \quad (31)$$

Here, $A_{R_x}[m, l] = \sum_{n=0}^{N-1} R_x[n] R_x^*[n - m] e^{-j2\pi ln/N}$ is the ambiguity function of the correlation $R_x[m]$. The relation (30) suggests the following "data-driven" estimator of $R_L[rM, sN/M]$:

$$\hat{R}_{L,\mathrm{d}}\left[rM, s\frac{N}{M}\right] \triangleq \frac{\hat{A}_{y_f}\left[rM, s\frac{N}{M}\right] - \alpha\delta[r]\delta[s]}{\frac{N_f^2 N}{M} A_{R_x}\left[0, s\frac{N}{M}\right]}$$
$$= \frac{M}{N_f^2 N} \frac{\hat{A}_{y_f}\left[rM, s\frac{N}{M}\right]}{A_{R_x}\left[0, s\frac{N}{M}\right]} - \frac{M}{N_f^2 N} \frac{\alpha\delta[r]\delta[s]}{E_{R_x}} \quad (32)$$

in which

$$\hat{A}_{y_f}\left[rM, s\frac{N}{M}\right] = \frac{1}{L} \sum_{i=0}^{L-1} A_{y_f^{(i)}}\left[rM, s\frac{N}{M}\right]$$

is an estimate of $\bar{A}_{y_f}[rM, sN/M]$ that uses L filterbank output signals $y_f^{(i)}[n]$, and $E_{R_x} = A_{R_x}[0,0] = \sum_{n=0}^{N-1} |R_x[n]|^2$. As a difference from the estimator in (18), each $y_f^{(i)}[n]$ is obtained by *data-driven* channel sounding according to (29) (i.e., using the matched receive filterbank with noise-suppression windowing). It is assumed that N_0, $R_x[m]$, and the path loss $R_L[0,0]$ are known or have been estimated.[3]

Finally, from $\hat{R}_{L,\mathrm{d}}[rM, sN/M]$, a corresponding data-driven SF estimator is obtained via a 2-D DFT, which yields [cf. (20)]

$$\hat{C}_{\mathrm{d}}[m, l] = \frac{M}{N_f^2} \sum_{r=0}^{\frac{N}{M}-1} \sum_{s=0}^{M-1} \frac{\hat{A}_{y_f}\left[rM, s\frac{N}{M}\right]}{A_{R_x}\left[0, s\frac{N}{M}\right]} \times e^{-j2\pi\left(\frac{lr}{\frac{N}{M}} - \frac{ms}{M}\right)} - \alpha M / N_f^2 N E_{R_x}. \quad (33)$$

Again, the Zak transform allows the efficient computation of $\hat{A}_{y_f}[rM, sN/M]$ [cf. (25)], and a "subsubsampled" estimator can be used for strongly underspread channels (cf. Section IV-D).

[3]Experiments indicate that for typical receive filter lengths N_f, the data-driven estimator is quite insensitive to errors in estimating $R_L[0, 0]$.

C. Bias/Variance Analysis

We now analyze the bias and variance of the data-driven estimator $\hat{C}_{\mathrm{d}}[m,l]$ in (33). We will neglect the commutation error caused by imperfect commutation of channel H and receive filters f_r.

Bias: With $\mathbb{E}\{\hat{A}_{y_f}[m,l]\} = \bar{A}_{y_f}[m,l]$ and using (30), it easily follows that $\hat{C}_{\mathrm{d}}[m,l]$ *is unbiased*, i.e., $\mathbb{E}\{\hat{C}_{\mathrm{d}}[m,l]\} \equiv C[m,l]$.

Variance: We first consider the conditional variance of $\hat{C}_{\mathrm{d}}[m,l]$ given the data (sounding) signal $x[n]$. We assume that i) $h[n,m]$ and $w[n]$ are statistically independent, circularly symmetric, complex Gaussian processes; ii) successive channel soundings are separated by at least the channel's coherence time [2] so that all channel measurements are statistically independent; iii) the noise-suppression window is rectangular: $g[n] = \mathrm{rect}_M[n - N_{R_x}]$; and iv) $N_f + N_{R_x} \leq M$ and $2N_{R_x} + N_m < M$. We will neglect errors resulting from imperfect estimates of the correlation function, i.e., we formally set $\hat{R}_x^{(r)}[m] = R_x[m]$ (this can be expected to be approximately true if N_f is not too small). One can then show by means of a rather tedious calculation that the average conditional variance of $\hat{C}_{\mathrm{d}}[m,l]$ given $x[n]$ is bounded as

$$V_x \triangleq \frac{1}{N}\sum_{m=0}^{M-1}\sum_{l=0}^{\frac{N}{M}-1}\mathrm{var}\left\{\hat{C}_{\mathrm{d}}[m,l]|x[n]\right\}$$

$$\leq \frac{\eta E_{R_x}}{L}\sum_{s=0}^{M-1}\frac{1}{\left|A_{R_x}\left[0,s\frac{N}{M}\right]\right|^2}$$

with

$$\eta \triangleq \frac{E_{R_x}\|C\|^2\left(4N_{R_x}+1\right)}{NM} + \frac{N^2}{N_f^2}[E_{R_x}R_L^2[0,0]\left(4N_{R_x}+1\right)\left(2N_f+M\right) + 2P_xN_0R_L[0,0]\left(2N_{R_x}+1\right)\left(N_f+M\right)+N_0^2M]$$

where $P_x \triangleq R_x[0] = \mathbb{E}\{|x[n]|^2\}$ and $\|C\|^2 \triangleq \sum_{m=0}^{M-1}\sum_{l=0}^{N/M-1}C^2[m,l]$. It is seen that this bound on V_x does not depend on $x[n]$ (a consequence of our assumption $\hat{R}_x^{(r)}[m] = R_x[m]$); therefore, it is also a bound on the unconditional average variance $V = (1/N)\sum_{m=0}^{M-1}\sum_{l=0}^{N/M-1}\mathrm{var}\{\hat{C}_{\mathrm{d}}[m,l]\}$:

$$V \leq \frac{\eta E_{R_x}}{L}\sum_{s=0}^{M-1}\frac{1}{\left|A_{R_x}\left[0,s\frac{N}{M}\right]\right|^2}. \tag{34}$$

This variance bound decreases for increasing receive filter length N_f and increasing number L of soundings. It is minimum when $|A_{R_x}[0,sN/M] = \text{const}$; using variational calculus, it can be shown that this is the case if and only if $R_x[m] = \sigma_x^2\delta[m]$, i.e., if and only if $x[n]$ is *white*. Thus, nonwhite data signals must be expected to lead to a higher variance. It can also be shown that for $R_x[m] = \sigma_x^2\delta[m]$, the right-hand side in (34) is equal to the average variance V and not just a bound on V.

The overall structure of the variance bound (34) resembles that of the variance bound (27) for the SF estimator using dedicated sounding signals. However, the denominator in (27) ($|A_{x_v}[rM,sN/M]|^2$) is replaced by $|A_{R_x}[0,sN/M]|^2$. Thus, the variance bound of the data-driven estimator merely depends on the second-order statistics (correlation $R_x[m]$) of the data signal process $x[n]$.

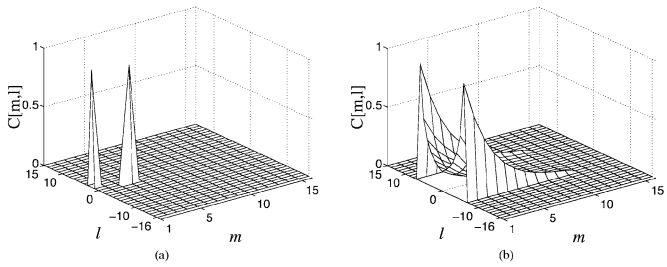

Fig. 2. SFs used for the simulations. (a) Two-path model. (b) Jakes/exponential model.

D. MMSE-Type Equalization

Together with the noise bias correction, the "zero-forcing equalization" corresponding to the division by $(N_f^2N/M)A_{R_x}[0,sN/M]$ in (32) causes $\hat{C}_{\mathrm{d}}[m,l]$ to be effectively unbiased for any $R_x[m]$. However, as was discussed above, this equalization must be expected to result in a larger variance if some values $A_{R_x}[0,sN/M]$ are small, i.e., if $x[n]$ is nonwhite. For variance reduction, we may consider a biased estimator

$$\hat{R}_{L,\mathrm{d,b}}\left[rM,s\frac{N}{M}\right] \triangleq \frac{\hat{A}_{y_f}\left[rM,s\frac{N}{M}\right]-\alpha\delta[r]\delta[s]}{D[s]}$$

from which an SF estimator $\hat{C}_{\mathrm{d,b}}[m,l]$ is obtained by means of a 2-D DFT as usual. The denominator $D[s]$ is chosen to minimize an upper bound on the MSE. Since the derivation of the optimum $D[s]$ is analogous to Section V-B, we just present the result:

$$D[s] = \frac{N_f^2N}{M}\frac{\left|A_{R_x}\left[0,s\frac{N}{M}\right]\right|^2+\frac{\eta E_{R_x}M}{N^3LR_L^2[0,0]}}{A_{R_x}^*\left[0,s\frac{N}{M}\right]} = \frac{N_f^2N}{M}A_{R_x}\left[0,s\frac{N}{M}\right] + \frac{\eta E_{R_x}N_f^2}{N^2LR_L^2[0,0]A_{R_x}^*\left[0,s\frac{N}{M}\right]}. \tag{35}$$

VII. Simulation Results

To assess the performance of the proposed SF estimators $\hat{C}[m,l]$ in (20) and $\hat{C}_{\mathrm{d}}[m,l]$ in (33), we simulated synthetic WSSUS channels with i) an SF corresponding to a two-path channel with $N_m = 4$, $N_l = 3$ and ii) the classical Jakes/exponential SF [19] with $N_m = 11$, $N_l = 13$ (see Fig. 2). We used the parameters $N = 510$ and $M = 15$, unless stated otherwise; note that (8) is always satisfied. The spreading factor was $N_mN_l/N = 0.024$ for the two-path channel and $N_mN_l/N = 0.32$ for the Jakes/exponential channel (except for the last simulation). Because of its large spreading factor, the Jakes/exponential channel is a difficult test case for all algorithms.

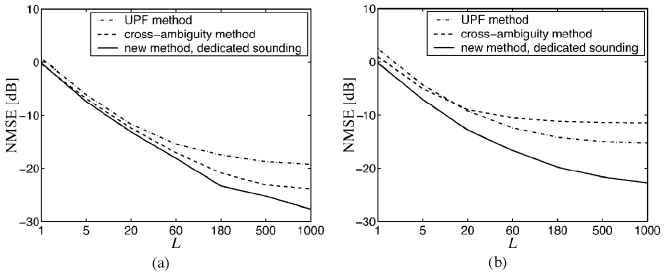

Fig. 3. Comparison of proposed SF estimator $\hat{C}[m,l]$ versus UPF and cross-ambiguity methods for the noise-free case: NMSE versus L for (a) two-path SF and (b) Jakes/exponential SF.

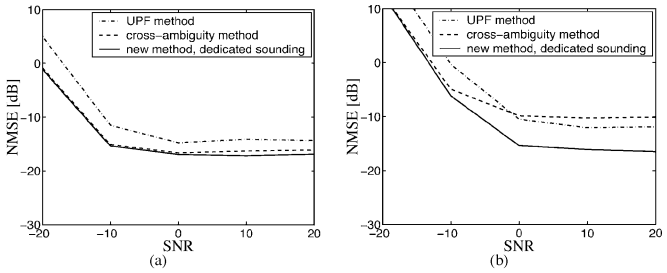

Fig. 4. Comparison of proposed SF estimator $\hat{C}[m,l]$ versus UPF and cross-ambiguity methods with noise for $L = 50$. NMSE versus SNR for (a) two-path SF and (b) Jakes/exponential SF.

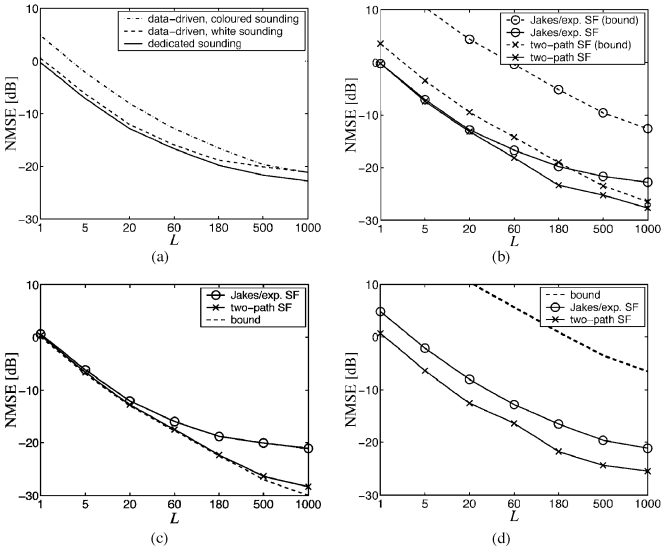

Fig. 5. Comparison of simulated NMSEs and normalized MSE bounds for the noise-free case. (a) $\hat{C}[m,l]$ and $\hat{C}_{\rm d}[m,l]$ for Jakes/exponential SF. (b) $\hat{C}[m,l]$ and normalized bound (27). (c) $\hat{C}_{\rm d}[m,l]$ and normalized bound (34) using white data signal ($N_{R_x} = 0$). (d) $\hat{C}_{\rm d}[m,l]$ and normalized bound (34) using colored data signal ($N_{R_x} = 2$). In (b)–(d), a solid line indicates the simulated NMSE, whereas a dashed line indicates the corresponding bound. Note that in (c) and (d), the bound is independent of the SF.

For the estimator $\hat{C}[m,l]$, the sounding pulse $g[n]$ in (9) was a maximum-length pseudonoise sequence of length $M = 15$. Unless indicated otherwise, the receive filter $f[n]$ was matched to $g[n]$ (thus, $N_f = 15$). For the data-driven estimator $\hat{C}_{\rm d}[m,l]$, the data signal was white or colored stationary Gaussian noise with unit variance (this type of signal approximates the transmit signals arising e.g. in OFDM).

Simulation Study 1: First, we present a performance comparison of our SF estimator $\hat{C}[m,l]$ with an improved version of the cross-ambiguity estimator[4] proposed in [13] and the uncertainty product function (UPF) estimator [15]. The cross-ambiguity estimator used a maximum-length pseudonoise sequence of length 511 as sounding signal. The UPF estimator used two maximum-length pseudonoise sequences of length 511. For the noise-free case, and for each of the three methods, Fig. 3 shows the estimated[5] average normalized MSE (NMSE) $\mathbb{E}\{\|\hat{C}-C\|^2\}/\|C\|^2$ versus L (the number of soundings). The NMSE of $\hat{C}[m,l]$ is seen to initially decay with increasing L according to $1/L$, as suggested by the variance bound (27). However, for larger values of L, the NMSE decay levels off. This is due to the commutation error that cannot be reduced by more averaging. The commutation error can be reduced by using a shorter receive filter length N_f; however, this comes at the cost of a higher variance (see simulation study 3).

Fig. 4 shows the effects of noise. The NMSE is plotted versus the SNR for a fixed number $L = 50$ of soundings. (The SNR is defined as $(1/N)\sum_{n=0}^{N-1}\mathbb{E}\{|y[n]|^2\}/N_0$.) It can be seen that for low SNR, the NMSE drops rapidly with increasing SNR since here, the noise is the dominating source of error. For higher SNR, the curves level off since the dominating source of error now is the randomness of the channel. Comparing Fig. 4(a) and (b), it can be seen that the NMSE is higher for the (more complicated) Jakes/exponential SF than for the (simpler) two-path SFs.

It is seen that in all cases, the proposed estimator $\hat{C}[m,l]$ performs better than the UPF and cross-ambiguity estimators. This improvement is especially pronounced for larger values of L, i.e., when more averaging is used, and for more complicated SFs (Jakes/exponential SF) where the UPF and cross-ambiguity estimators suffer from "self-clutter." It is furthermore seen that the NMSE performance of the proposed estimator $\hat{C}[m,l]$ and of the UPF estimator is less dependent on the shape of the SF than that of the cross-ambiguity estimator. Indeed, the cross-ambiguity estimator introduces more self-clutter, which results in a larger bias when the channel contains more scatterers. In contrast, the self-clutter of the UPF estimator seems to be relatively independent of the shape of the SF.

Simulation Study 2: In Fig. 5, the NMSE of our SF estimators $\hat{C}[m,l]$ and $\hat{C}_{\rm d}[m,l]$ and the corresponding MSE/variance bounds[6] (again normalized by $||C||^2$) are considered for the noise-free case. Fig. 5(a) compares the performance of $\hat{C}[m,l]$ and $\hat{C}_{\rm d}[m,l]$ (the latter both for a white data/sounding signal $x[n]$ and for a colored $x[n]$ with $N_{R_x} = 2$) for the Jakes/exponential SF. The receive filter length for $\hat{C}_{\rm d}[m,l]$ was chosen as $N_f = 14$ for white $x[n]$ and $N_f = 12$ for colored $x[n]$ (the maximum values of N_f such that $N_f + N_{R_x} \leq M$ is satisfied, cf. Section VI-B). It is seen that $\hat{C}_{\rm d}[m,l]$ with white $x[n]$ performs almost as well as $\hat{C}[m,l]$, whereas a colored $x[n]$ results in a significantly higher NMSE.

[4]The improvement corresponds to a noise bias correction that is analogous to the subtraction of $\bar{A}_{w_f}[\Delta n, \Delta k]$ in (14).

[5]The MSE was estimated by averaging over 20 to 2000 simulation runs (depending on the number of soundings).

[6]Note that the variance bounds in (27) and (34) are simultaneously MSE bounds because the estimators are unbiased.

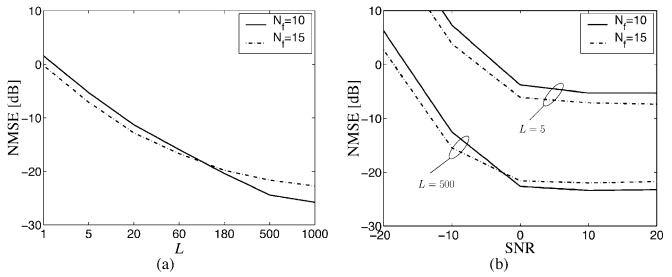

Fig. 6. Performance of $\hat{C}[m,l]$ for receive filter lengths $N_f = 15$ and $N_f = 10$ (Jakes/exponential SF). (a) NMSE versus L for the noise-free case. (b) NMSE versus SNR for $L = 5$ and $L = 500$.

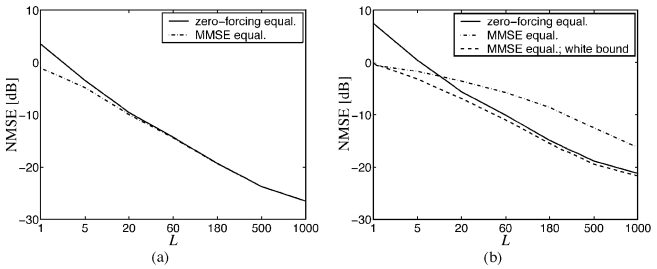

Fig. 7. NMSE comparison of the data-driven SF estimators with conventional ("zero-forcing") equalization $\hat{C}_{\mathrm{d}}[m,l]$ and with MMSE equalization $\hat{C}_{\mathrm{d,b}}[m,l]$ for the two-path SF and an SNR of -12 dB. (a) White sounding signal. (b) Colored sounding signal with $N_{R_x} = 2$.

Fig. 5(b) compares the NMSE of $\hat{C}[m,l]$ with the corresponding (normalized) MSE bound (27) for both the Jakes/exponential SF and the two-path SF. It is seen that the bound increasingly overestimates the NMSE with increasing complexity of the SF (i.e., increasing number of scatterers). Fig. 5(c) compares the NMSE of $\hat{C}_{\mathrm{d}}[m,l]$ with the bound (34) using a white data signal $x[n]$ ($N_{R_x} = 0$). It is seen that the bound is in fact slightly *smaller* than the actual (estimated) NMSE. Evidently, the assumptions underlying the bound (perfect commutation, equality $\hat{R}_x^{(r)}[m] = R_x[m]$) are not satisfied sufficiently well. Finally, Fig. 5(d) shows the results obtained for a colored data signal ($N_{R_x} = 2$); it can be seen that the bound is much less tight in this case.

Simulation Study 3: Next, we investigate the effect of different receive filter lengths $N_f = 15$ and $N_f = 10$ on the performance of $\hat{C}[m,l]$ for the Jakes/exponential SF. Fig. 6(a) shows the NMSE versus the number of soundings L for the noise-free case. It is seen that for small L, the shorter length $N_f = 10$ results in a higher variance and, thus, initially in a higher NMSE. For L large, however, the commutation error becomes dominant, and the NMSE obtained with $N_f = 10$ drops below that obtained with $N_f = 15$.

Fig. 6(b) shows the NMSE versus SNR for $L = 5$ and $L = 500$ soundings. As expected, for $L = 5$, the larger receive filter length $N_f = 15$ always performs better because the error due to the noise and channel randomness is dominant as compared with the commutation error. For $L = 500$, however, the smaller receive filter length $N_f = 10$ performs better above an SNR level of about -2 dB.

Simulation Study 4: Fig. 7(a) compares the results of the data-driven SF estimator ($\hat{C}_{\mathrm{d}}[m,l]$) and the data-driven SF estimator with MMSE equalization proposed in Section VI-D ($\hat{C}_{\mathrm{d,b}}[m,l]$). We used the two-path SF and a low SNR of -12 dB (the benefits of MMSE equalization are greatest at low SNR). The data (sounding) signal was white. It can be observed that the MMSE equalization leads to an improvement over the "zero-forcing" (ZF) equalization employed by $\hat{C}_{\mathrm{d}}[m,l]$ if the number of soundings L is small, whereas for larger L, there is little or no improvement.

Fig. 7(b) compares the results obtained with $\hat{C}_{\mathrm{d}}[m,l]$ and $\hat{C}_{\mathrm{d,b}}[m,l]$ for a colored sounding signal with $N_{R_x} = 2$. The results of MMSE equalization using the variance bound for a white sounding signal (even though the sounding signal was colored) are also shown. This is motivated by the fact that the bound for a white sounding signal approximates the observed NMSE better than the bound for a colored sounding signal [see Fig. 5(c) and (d)]. In fact, it can be seen that for L sufficiently large, the looseness of the "colored" bound causes the MMSE method to have poorer performance than the ZF method, whereas using the "white" bound, the MMSE method performs consistently better than the ZF method.

Further experiments showed that MMSE equalization works well for simple SFs (i.e., a small number of scatterers). However, for a larger number of scatterers, the bias bound that is used to calculate (35) becomes loose so that its influence on $D[s]$ is too large. As a consequence, the performance of MMSE equalization tends toward that of ZF equalization, even for small L. Our experiments suggest that this problem can be alleviated by replacing (35) with

$$D[s] = \frac{N_f^2 N}{M} A_{R_x}\left[0, s\frac{N}{M}\right] + \frac{N_s \eta E_{R_x} N_f^2}{N^2 L R_L^2[0,0] A_{R_x}^*[0, s\frac{N}{M}]}$$

where N_s is the effective number of scatterers.

Simulation Study 5: We finally present a performance comparison of $\hat{C}[m,l]$ with the averaged periodogram estimator $\hat{C}_{\mathrm{per}}[m,l]$ in (23) for the noise-free case and dedicated sounding signals. Motivated by the parameters of a UMTS system (e.g. [37]), we chose a carrier frequency of 2 GHz. The channel had a Jakes/exponential SF with maximum (one-sided) Doppler shift $B_D = 600$ Hz (corresponding to maximum velocity 324 km/h) and maximum delay $\tau_{\max} = 3.3$ μs. This channel is strongly underspread ($\tau_{\max} B_D = 0.004 \ll 1$). We used a sampling frequency of $f_s = 3.84$ MHz (the chip rate of UMTS) and a sounding duration of about 10 ms (corresponding to a UMTS frame). This resulted in $N_m = 11$ and $N_l = 13$. We chose $N = 38\,354$ and $M = 127$ [note that N is a multiple of M, and (8) is satisfied]. There were approximately 100 soundings/s. The sounding pulse was a maximum-length pseudonoise sequence of length $M = 127$ convolved by a filter with impulse response [0.3, 1, 0.3] that accounts for imperfections such as bandlimitation, nonideal pulse-shaping, etc. At the receiver, a matched filter of length $N_f = 127$ was used.

Fig. 8 shows the NMSE of $\hat{C}[m,l]$ and $\hat{C}_{\mathrm{per}}[m,l]$ versus L. (We did not consider the cross-ambiguity and UPF methods because their computational complexity is excessive for the large block length used in this example.) It is seen that for growing L, the NMSE of $\hat{C}_{\mathrm{per}}[m,l]$ saturates at about -15 dB due to the bias resulting from the nonideal sounding pulse. In contrast,

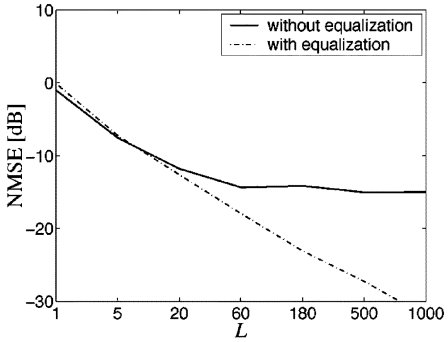

Fig. 8. NMSE comparison of $\hat{C}[m,l]$ ("with equalization") and the averaged periodogram estimator $\hat{C}_{\rm per}[m,l]$ ("without equalization") for the Jakes/exponential SF in the noise-free case.

$\hat{C}[m,l]$ is effectively unbiased and, thus, features no such saturation effect; it outperforms $\hat{C}_{\rm per}[m,l]$ for more than about ten soundings.

VIII. Conclusion

We have presented two novel methods for the estimation of the scattering function (SF) of *underspread* WSSUS channels. The underspread property is practically relevant since it is satisfied by usual mobile radio channels, even when they are fast time-varying. The proposed methods exploit the fact that due to the underspread property, it suffices to estimate the channel's time-frequency correlation function on a subsampled lattice. This was seen to have two beneficial effects. First, the requirements on the (virtual) sounding signal are significantly relaxed since its ambiguity function needs to be approximately constant only on the subsampled lattice. Second, the subsampling allows the use of an efficient implementation based on the Zak transform. Especially for large block length N, our methods have significantly lower computational complexity than the alternative methods proposed in [13]–[17].

The proposed SF estimators use a "noise bias correction" as well as an "equalization" that compensates for systematic imperfections of the sounding signal. These measures cause the estimators to be effectively unbiased. The "equalization" tends to increase the estimation variance that, however, can be made arbitrarily small by a sufficient number of soundings (i.e., averaging).

One of our estimators requires an explicit sounding phase during which no data can be transmitted. The sounding signal can be freely chosen to optimize sounding results. The other estimator uses the data signal itself as an implicit sounding signal. This "data-driven" SF estimator allows a continuous estimation (monitoring) of the SF during an ongoing data transmission, without an explicit sounding phase. This is made possible by a *matched receive filterbank* that emulates an admissible sounding signal.

Simulation results demonstrated that the performance of the proposed SF estimators is typically superior to that of existing nonparametric methods. This superiority is especially pronounced in challenging situations (fast time-varying channels, poor sounding signals, low SNR). A performance and complexity comparison of our SF estimators with the parametric (AR model based) SF estimator proposed in [18] would be an interesting topic for future research.

Appendix A
Discretization of Continuous-Time LTV Channels

Our discussion of the discretization of a continuous-time LTV channel extends the results reported in [1] and [28] to the discrete-time case [38]. The (equivalent complex baseband) input–output relation of a continuous-time LTV channel $\boldsymbol{H}_c$ with impulse response $\tilde{h}_c(t,\tau)$ is

$$y(t) = (\boldsymbol{H}_c x)(t) = \int_{-\infty}^{\infty} \tilde{h}_c(t,\tau) x(t-\tau) d\tau. \qquad (36)$$

We assume the following.

1) The input signal $x(t)$ is bandlimited with bandwidth B, i.e., $X(f) = 0$ for $|f| > B$. With (36), one can then show that without loss of generality, the impulse response $\tilde{h}_c(t,\tau)$ can be replaced by a version $h_c(t,\tau)$ that is bandlimited with respect to τ with the same bandwidth B [21].
2) The impulse response $h_c(t,\tau)$ is causal and delay-limited with maximum delay $\tau_{\max}$, i.e., $h_c(t,\tau) = 0$ for $\tau \notin [0,\tau_{\max}]$. (This assumption is not *exactly* compatible with the bandlimitation of $h_c(t,\tau)$ with respect to τ; the resulting errors will, however, be ignored.)
3) The channel's Doppler shifts are limited to $[-B_D, B_D]$, which implies that the impulse response $h_c(t,\tau)$ is bandlimited with respect to t with bandwidth B_D.
4) We are interested in the output signal $y(t)$ only in the interval [0,$t_{\max}$], with $t_{\max} > \tau_{\max}$. This corresponds to a blockwise processing of the channel output, which is well suited to many digital communication schemes. The truncation with respect to t corresponds to a smoothing (resolution loss) in the Doppler direction and allows the SF to be sampled in the Doppler direction. The maximum allowable sampling period is determined by the block length $t_{\max}$.

Based on these assumptions, the channel $\boldsymbol{H}_c$ can be discretized as follows. Because $h_c(t,\tau)$ is bandlimited with respect to τ, it can be represented using the samples $h_c(t,m/f_i)$ according to

$$h(t,\tau) = \sum_{m=0}^{N_m-1} h_c\left(t,\frac{m}{f_i}\right) \operatorname{sinc}\left(\pi f_i\left(\tau-\frac{m}{f_i}\right)\right) \qquad (37)$$

with $\operatorname{sinc}(\alpha) = \sin(\alpha)/\alpha$, "input" sampling frequency $f_i \geq 2B$, and $N_m = \lfloor \tau_{\max} F_i \rfloor + 1$. Inserting (37) into (36) and interchanging the order of integration and summation yields

$$\begin{aligned} y(t) &= \sum_{m=0}^{N_m-1} h_c\left(t,\frac{m}{f_i}\right) \int_{-\infty}^{\infty} \operatorname{sinc}\left(\pi f_i\left(\tau-\frac{m}{f_i}\right)\right) x(t-\tau) d\tau \\ &= \frac{1}{f_i} \sum_{m=0}^{N_m-1} h_c\left(t,\frac{m}{f_i}\right) x\left(t-\frac{m}{f_i}\right) \end{aligned}$$

where for the last equation, assumption 1 has been used. With assumptions 1 and 3, it can be shown (e.g. [1]) that the output signal $y(t)$ is bandlimited with bandwidth $B + B_D$; thus, it can

be sampled without loss of information using the "output" sampling frequency $f_o \geq 2(B+B_D)$. This yields

$$y\left(\frac{n}{f_o}\right)=\frac{1}{f_i}\sum_{m=0}^{N_m-1} h_c\left(\frac{n}{f_o},\frac{m}{f_i}\right)x\left(\frac{n}{f_o}-\frac{m}{f_i}\right),\ \ n\in[0,N-1] \tag{38}$$

with the *block length* $N=\lfloor t_{\max}f_o\rfloor+1$ (cf. assumption 4).

For simplicity, we hereafter use one common sampling frequency $f_s=f_i=f_o=2(B+B_D)$. (This means that the input signal is oversampled by a factor of $1+B_D/B$.) Then, (38) can be compactly written as

$$y[n]=\sum_{m=0}^{N_m-1} h[n,m]x[n-m],\quad n\in[0,N-1]$$

with $y[n]\triangleq y(n/f_s)$, $x[n]\triangleq x(n/f_s)$, and $h[n,m]\triangleq(1/f_s)h_c(n/f_s,m/f_s)$. This is the input–output relation of a *discrete-time* LTV channel $\boldsymbol{H}$ that provides a discrete-time representation of the original continuous-time LTV channel $\boldsymbol{H}_c$. Due to assumption 2, the impulse response $h[n,m]$ is zero for $m\notin[0,N_m-1]$. Moreover, due to assumption 4, we can consider $h[n,m]$ to be zero for $n\notin[0,N-1]$. Thus

$$h[n,m]=0\quad \text{for } (n,m)\notin[0,N-1]\times[0,N_m-1]$$
$$\text{with } N=\lfloor t_{\max}f_s\rfloor+1,\quad N_m=\lfloor \tau_{\max}f_s\rfloor+1.$$

We finally assume that $x[n]=0$ for $n\notin[0,N_x-1]$. Then, to be able to discretize the Doppler shift variable (cf. Section II-A) without temporal aliasing of the output signal $y[n]$ on the interval [0, $N-1$], we have to suppose that $t_{\max}$ is chosen such that $N\geq N_x+N_m-1$ (see [38] for details).

Appendix B
Derivation of (27)

We outline the derivation of the upper bound (27) on the average variance of the SF estimator $\hat{C}[m,l]$ in (19). With (18), the variance of $\hat{C}[m,l]$ is

$$\operatorname{var}\left\{\hat{C}[m,l]\right\}$$
$$=N^2\operatorname{var}\left\{\sum_{r=0}^{\frac{N}{M}-1}\sum_{s=0}^{M-1}\frac{\hat{A}_{y_f}\left[rM,s\frac{N}{M}\right]-NN_0r_f[rM]\delta[s]}{A_{x_v}\left[rM,s\frac{N}{M}\right]}\times e^{-j2\pi\left(\frac{lr}{N/M}-\frac{ms}{M}\right)}\right\}.$$

It is then easily shown that the *average* variance $V=(1/N)\sum_{m=0}^{M-1}\sum_{l=0}^{N/M-1}\operatorname{var}\{\hat{C}[m,l]\}$ is given by

$$V=N^2\sum_{r=0}^{\frac{N}{M}-1}\sum_{s=0}^{M-1}\frac{\mathbb{E}\left\{\left|A_{y_f}\left[rM,s\frac{N}{M}\right]\right|^2\right\}}{\left|A_{x_v}\left[rM,s\frac{N}{M}\right]\right|^2}-N^2\sum_{r=0}^{\frac{N}{M}-1}\sum_{s=0}^{M-1}\frac{\left|\bar{A}_{y_f}\left[rM,s\frac{N}{M}\right]\right|^2}{\left|A_{x_v}\left[rM,s\frac{N}{M}\right]\right|^2}.$$

Under the assumptions stated in Section V-A (i.e., $h[n,m]$ and $w[n]$ are circularly symmetric complex Gaussian processes and the $y_f^{(i)}[n]$ are statistically independent), we can use Isserlis' relation[7] [39], [40] and obtain after some calculations

$$V=\frac{N}{L}\sum_{r=0}^{\frac{N}{M}-1}\sum_{s=0}^{M-1}\sum_{m=0}^{N-1}\sum_{l=0}^{N-1}\frac{\left|\bar{A}_{y_f}[m,l]\right|^2}{\left|A_{x_v}\left[rM,s\frac{N}{M}\right]\right|^2}e^{-j2\pi\left(\frac{ms}{M}-\frac{lr}{N/M}\right)}. \tag{39}$$

With our further assumption that $h[n,m]$ and $w[n]$ are statistically independent, we can use (13) and obtain

$$\left|\bar{A}_{y_v}[m,l]\right|^2=|R_L[m,l]|^2\left|A_{x_v}[m,l]\right|^2+\left|\bar{A}_{w_f}[m,l]\right|^2+2\operatorname{Re}\left\{R_L[m,l]A_{x_v}[m,l]\bar{A}^*_{w_f}[m,l]\right\}$$

where in our case, $\bar{A}_{w_f}[m,l]=NN_0r_f[m]\delta[l]$. Assuming that commutation errors can be neglected, we can replace $|\bar{A}_{y_v}[m,l]|^2$ with $|\bar{A}_{y_f}[m,l]|^2$. Insertion of the above expression into (39) then yields

$$V=V_{\rm ch}+V_{\rm n}+V_{\rm mix} \tag{40}$$

with a channel term $V_{\rm ch}$, a noise term $V_{\rm n}$, and a mixed term $V_{\rm mix}$. The channel term is shown in the first equation at the bottom of the next page, where we used $|A_{x_v}[n,k]|^2\leq E^2_{x_v}$. The noise term is ($F[k]$ denotes the length-N DFT of $f[n]$)

$$\begin{aligned}V_{\rm n}&=\frac{N}{L}\sum_{r=0}^{\frac{N}{M}-1}\sum_{s=0}^{M-1}\sum_{m=0}^{N-1}\sum_{l=0}^{N-1}\frac{|NN_0r_f[m]\delta[l]|^2}{\left|A_{x_v}\left[rM,s\frac{N}{M}\right]\right|^2}\times e^{-j2\pi\left(\frac{ms}{M}-\frac{lr}{N/M}\right)}\\&=\frac{N^2N_0^2}{L}\sum_{r=0}^{\frac{N}{M}-1}\sum_{s=0}^{M-1}\sum_{k=0}^{N-1}\frac{|F[k]|^2\left|F\left[k-s\frac{N}{M}\right]\right|^2}{\left|A_{x_v}\left[rM,s\frac{N}{M}\right]\right|^2}\\&\leq\frac{N^2N_0^2}{L}\left[\sum_{k=0}^{N-1}|F[k]|^4\right]\sum_{r=0}^{\frac{N}{M}-1}\sum_{s=0}^{M-1}\frac{1}{\left|A_{x_v}\left[rM,s\frac{N}{M}\right]\right|^2}\end{aligned}$$

where the Schwarz inequality has been used. Finally, the mixed term is shown in the second equation at the bottom of the next page, where $|F[k]|^2\leq|F[k]|^2_{\max}$ has been used. Inserting the above bounds for $V_{\rm ch}$, $V_{\rm n}$, and $V_{\rm mix}$ in (40), we obtain the bound (27).

Appendix C
Derivation of (30)

We sketch the derivation of the "statistical input/output relation" (30). Our starting point is

$$\bar{A}_{y_f}\left[rM,s\frac{N}{M}\right]=\mathbb{E}\left\{\sum_{n=0}^{N-1}y_f[n]y_f^*[n-rM]e^{-j2\pi\frac{nsN/M}{N}}\right\}.$$

We now insert (29) and use Isserlis' relation (cf. Appendix B). Under the assumptions stated in Section VI-B (specifically,

[7]That is, $\mathbb{E}\{x_1x_2^*x_3^*x_4\}=\mathbb{E}\{x_1x_2^*\}\mathbb{E}\{x_3^*x_4\}+\mathbb{E}\{x_1x_3^*\}\mathbb{E}\{x_2^*x_4\}$ for zero-mean, circularly symmetric complex, jointly Gaussian random variables x_1, x_2, x_3 and x_4.

channel H and receive filters f_r commute perfectly; $x[n]$, $h[n,m]$, and $w[n]$ are circularly symmetric complex Gaussian and statistically independent; $R_x[m]=0$ for $|m|>N_{R_x}$ with $N_{R_x}\le\lfloor M/2\rfloor$ and $N_f+N_{R_x}\le M$), it is possible to derive

$$\bar{A}_{y_f}\left[rM,s\frac{N}{M}\right]=\sum_{n=0}^{N-1}\sum_{r'=0}^{\frac{N}{M}-1}\left[D[n,r,r']+\left(E+N_fN_0R_x[0]\right)\delta[r]\right]\left|g[n-r'M]\right|^2e^{-j2\pi\frac{ns}{M}} \tag{41}$$

where

$$D[n,r,r']\triangleq N_f^2\sum_{m=0}^{N_m-1}\left|R_x[n-m-r'M]\right|^2R_h[rM,m]$$

$$E\triangleq R_L[0,0]\sum_{m=-N_f+1}^{N_f-1}\left|R_x[m]\right|^2\left(N_f-|m|\right).$$

Using the further assumption that $\sum_{r=0}^{N/M-1}|g[n-rM]|^2\equiv c$ and $g[n]=1$ for $n\in[-N_{R_x},N_{R_x}+N_m-1]$ (i.e., $g[n]$ passes the desired signal components unscaled and undistorted), one can simplify (41) to

$$\begin{aligned}\bar{A}_{y_f}&\left[rM,s\frac{N}{M}\right]\\&=N_f^2\sum_{n=0}^{N-1}\sum_{r'=0}^{\frac{N}{M}-1}\sum_{m=0}^{N_m-1}\left|R_x[n-m-r'M]\right|^2R_h[rM,m]\times e^{-j2\pi\frac{ns}{M}}+\alpha\delta[r]\delta[s]\\&=\frac{N_f^2}{N^2}\sum_{n=0}^{N-1}\sum_{k=0}^{N-1}\sum_{l=0}^{N-1}\sum_{r'=0}^{\frac{N}{M}-1}\sum_{m=0}^{N_m-1}A_{R_x}[0,l]R_L[rM,k]\times e^{j2\pi\frac{-ns\frac{N}{M}+km+l(n-m-r'M)}{N}}+\alpha\delta[r]\delta[s]\\&=\frac{N_f^2N}{M}A_{R_x}\left[0,s\frac{N}{M}\right]R_L\left[rM,s\frac{N}{M}\right]+\alpha\delta[r]\delta[s]\end{aligned}$$

which is (30) [α is defined as in (31)].

ACKNOWLEDGMENT

The authors would like to thank H. Bölcskei for suggesting the use of the Zak transform.

$$\begin{aligned}V_{\text{ch}}&=\frac{N}{L}\sum_{r=0}^{\frac{N}{M}-1}\sum_{s=0}^{M-1}\sum_{m=0}^{N-1}\sum_{l=0}^{N-1}\frac{\left|R_L[m,l]\right|^2\left|A_{x_v}[m,l]\right|^2}{\left|A_{x_v}\left[rM,s\frac{N}{M}\right]\right|^2}e^{-j2\pi\left(\frac{ms}{M}-\frac{lr}{N/M}\right)}\\&=\frac{1}{N}\sum_{r=0}^{\frac{N}{M}-1}\sum_{s=0}^{M-1}\sum_{m=0}^{N-1}\sum_{l=0}^{N-1}\sum_{m'=0}^{N-1}\sum_{l'=0}^{N-1}\frac{C\left[m'+rM-m,l'+s\frac{N}{M}-l\right]C[m',l']\left|A_{x_v}[m,l]\right|^2}{\left|A_{x_v}\left[rM,s\frac{N}{M}\right]\right|^2}\\&\le\frac{E_{x_v}^2}{N^2}\sum_{r=0}^{\frac{N}{M}-1}\sum_{s=0}^{M-1}\sum_{m'=0}^{N-1}\sum_{l'=0}^{N-1}\frac{C[m',l']}{\left|A_{x_v}\left[rM,s\frac{N}{M}\right]\right|^2}\sum_{m=0}^{N-1}\sum_{l=0}^{N-1}C\left[m'+rM-m,l'+s\frac{N}{M}-l\right]\\&=\frac{E_{x_v}^2}{N^2}\sum_{r=0}^{\frac{N}{M}-1}\sum_{s=0}^{M-1}\sum_{m=0}^{N-1}\sum_{l=0}^{N-1}\frac{C[m,l]}{\left|A_{x_v}\left[rM,s\frac{N}{M}\right]\right|^2}N^2R_L[0,0]\\&=N^2E_{x_v}^2R_L^2[0,0]\sum_{r=0}^{\frac{N}{M}-1}\sum_{s=0}^{M-1}\frac{1}{\left|A_{x_v}\left[rM,s\frac{N}{M}\right]\right|^2}\end{aligned}$$

$$\begin{aligned}V_{\text{mix}}&=\frac{N}{L}\sum_{r=0}^{\frac{N}{M}-1}\sum_{s=0}^{M-1}\sum_{m=0}^{N-1}\sum_{l=0}^{N-1}\frac{2\text{Re}\left\{R_L[m,l]A_{x_v}[m,l]NN_0r_f[m]\delta[l]\right\}}{\left|A_{x_v}\left[rM,s\frac{N}{M}\right]\right|^2}e^{-j2\pi\left(\frac{ms}{M}-\frac{lr}{N/M}\right)}\\&=\frac{N_0}{NL}\sum_{r=0}^{\frac{N}{M}-1}\sum_{s=0}^{M-1}\sum_{m=0}^{N-1}\sum_{l=0}^{N-1}\sum_{k=0}^{N-1}\frac{C[m,l]\left|X_v[k]\right|^2\left(\left|F\left[s\frac{N}{M}-l-k\right]\right|^2+\left|F\left[-s\frac{N}{M}-l-k\right]\right|^2\right)}{\left|A_{x_v}\left[rM,s\frac{N}{M}\right]\right|^2}\\&\le\frac{2N_0\left|F[k]\right|_{\max}^2}{NL}\sum_{r=0}^{\frac{N}{M}-1}\sum_{s=0}^{M-1}\frac{1}{\left|A_{x_v}\left[rM,s\frac{N}{M}\right]\right|^2}\sum_{m=0}^{N-1}\sum_{l=0}^{N-1}C[m,l]\sum_{k=0}^{N-1}\left|X_v[k]\right|^2\\&=\frac{2N^2N_0\left|F[k]\right|_{\max}^2}{L}R_L[0,0]E_{x_v}\sum_{r=0}^{\frac{N}{M}-1}\sum_{s=0}^{M-1}\frac{1}{\left|A_{x_v}\left[rM,s\frac{N}{M}\right]\right|^2}\end{aligned}$$

REFERENCES

[1] P. A. Bello, "Characterization of randomly time-variant linear channels," *IEEE Trans. Commun. Syst.*, vol. COM-11, pp. 360–393, 1963.

[2] R. S. Kennedy, *Fading Dispersive Communication Channels*. New York: Wiley, 1969.

[3] H. L. Van Trees, *Detection, Estimation, and Modulation Theory, Part III: Radar-Sonar Signal Processing and Gaussian Signals in Noise*. Malabar, FL: Krieger, 1992.

[4] Y. Li, L. Cimini, and N. Sollenberger, "Robust channel estimation for OFDM systems with rapid dispersive fading channels," *IEEE Trans. Commun.*, vol. 46, pp. 902–915, July 1998.

[5] D. Schafhuber, G. Matz, and F. Hlawatsch, "Predictive equalization of time-varying channels for coded OFDM/BFDM systems," in *Proc. IEEE GLOBECOM*, San Franscisco, CA, Nov. 2000, pp. 721–725.

[6] S. S. Soliman and R. A. Scholtz, "Synchronization over fading dispersive channels," *IEEE Trans. Commun.*, vol. 36, pp. 499–505, Apr. 1988.

[7] F. Adachi and J. D. Parsons, "Error rate performance of digital FM mobile radio with postdetection diversity," *IEEE Trans. Commun.*, vol. 37, pp. 200–210, Feb. 1989.

[8] V. Filimon, W. Kozek, W. Kreuzer, and G. Kubin, "LMS and RLS tracking analysis for WSSUS channels," in *Proc. IEEE ICASSP*, Minneapolis, MN, 1993, pp. III/348–III/351.

[9] V. G. Subramanian and B. Hajek, "Broad-band fading channels: signal burstiness and capacity," *IEEE Trans. Inform. Theory*, vol. 48, pp. 809–827, Apr. 2002.

[10] W. Kozek and A. F. Molisch, "Nonorthogonal pulseshapes for multicarrier communications in doubly dispersive channels," *IEEE J. Select. Areas Commun.*, vol. 16, pp. 1579–1589, Oct. 1998.

[11] D. Schafhuber, G. Matz, and F. Hlawatsch, "Pulse-shaping OFDM/BFDM systems for time-varying channels: ISI/ICI analysis, optimal pulse design, and efficient implementation," in *Proc. IEEE PIMRC*, Lisbon, Portugal, Sept. 2002, pp. 1012–1016.

[12] H. Bölcskei, R. Koetter, and S. Mallik, "Coding and modulation for underspread fading channels," in *Proc. IEEE ISIT*, Lausanne, Switzerland, June–July 2002.

[13] N. T. Gaarder, "Scattering function estimation," *IEEE Trans. Inform. Theory*, vol. IT-14, pp. 684–693, Oct. 1968.

[14] P. E. Green Jr., "Radar measurements of target scattering properties," in *Radar Astronomy*, J. V. Evans and T. Hagfors, Eds. New York: McGraw-Hill, 1968, ch. 1.

[15] D. W. Ricker and M. J. Gustafson, "A low sidelobe technique for the direct measurement of scattering functions," *IEEE J. Ocean. Eng.*, vol. 21, pp. 14–23, Jan. 1996.

[16] S. K. Mehta and E. L. Titlebaum, "A new method for measurement of the target and channel scattering functions using Costas arrays and other frequency hop signals," in *Proc. IEEE ICASSP*, Toronto, ON, Canada, Apr. 1991, pp. 1337–1340.

[17] ——, "New results of the twin processor method of measurement of the channel and/or scattering functions," in *Proc. IEEE ICASSP*, San Francisco, CA, Mar. 1992, pp. 545–548.

[18] S. M. Kay and S. B. Doyle, "Rapid estimation of the range-Doppler scattering function," *IEEE Trans. Signal Processing*, vol. 51, pp. 255–268, Jan. 2003.

[19] J. G. Proakis, *Digital Communications*, 3rd ed. New York: McGraw-Hill, 1995.

[20] W. Kozek, "On the transfer function calculus for underspread LTV channels," *IEEE Trans. Signal Processing*, vol. 45, pp. 219–223, Jan. 1997.

[21] G. Matz and F. Hlawatsch, "Time-frequency transfer function calculus (symbolic calculus) of linear time-varying systems (linear operators) based on a generalized underspread theory," *J. Math. Phys., Special Issue on Wavelet and Time-Frequency Analysis*, vol. 39, pp. 4041–4071, Aug. 1998.

[22] H. Artés, G. Matz, and F. Hlawatsch, "An unbiased scattering function estimator for fast time-varying channels," in *Proc. 2nd IEEE Workshop Signal Process. Adv. Wireless Commun.*, Annapolis, MD, May 1999, pp. 411–414.

[23] ——, "Unbiased scattering function estimation during data transmission," in *Proc. IEEE VTC Fall*, Amsterdam, The Netherlands, Sept. 1999, pp. 1535–1539.

[24] L. A. Zadeh, "Frequency analysis of variable networks," *Proc. IRE*, vol. 76, pp. 291–299, Mar. 1950.

[25] S. M. Kay, *Modern Spectral Estimation*. Englewood Cliffs, NJ: Prentice-Hall, 1988.

[26] G. Matz, A. F. Molisch, F. Hlawatsch, M. Steinbauer, and I. Gaspard, "On the systematic measurement errors of correlative mobile radio channel sounders," *IEEE Trans. Commun.*, vol. 50, pp. 808–821, May 2002.

[27] T. Kailath, "Measurements on time-variant communication channels," *IEEE Trans. Inform. Theory*, vol. IT-8, pp. 229–236, Sept. 1962.

[28] ——, "Sampling models for linear time-variant filters," Res. Lab. Electron., Mass. Inst. Technol., Cambridge, MA, Tech. Rep. 352, May 1959.

[29] P. C. Fannin, A. Molina, S. S. Swords, and P. J. Cullen, "Digital signal processing techniques applied to mobile radio channel sounding," *Proc. Inst. Elect. Eng. F*, vol. 138, pp. 502–508, Oct. 1991.

[30] P. J. Cullen, P. C. Fannin, and A. Molina, "Wide-band measurement and analysis techniques for the mobile radio channel," *IEEE Trans. Veh. Technol.*, vol. 42, pp. 589–603, Nov. 1993.

[31] J. D. Parsons, D. A. Demery, and A. M. D. Turkmani, "Sounding techniques for wideband mobile radio channels: a review," *Proc. Inst. Elect. Eng. I*, vol. 138, pp. 437–446, Oct. 1991.

[32] R. Tolimieri and M. An, *Time-Frequency Representations*. Boston, MA: Birkhäuser, 1998.

[33] M. I. Skolnik, *Introduction to Radar Systems*. New York: McGraw-Hill, 1980.

[34] C. E. Cook and M. Bernfeld, *Radar Signals—An Introduction to Theory and Applications*. Norwood, MA: Artech House, 1993.

[35] P. Stoica and R. Moses, *Introduction to Spectral Analysis*. Englewood Cliffs, NJ: Prentice-Hall, 1997.

[36] H. Bölcskei and F. Hlawatsch, "Discrete Zak transforms, polyphase transforms, and applications," *IEEE Trans. Signal Processing*, vol. 45, pp. 851–866, Apr. 1997.

[37] 3GPP, "TS 25.211. Physical channels and mapping of transport channels onto physical channels (FDD),", www.3gpp.org, vol. 3.2.0, Mar. 2000.

[38] H. Artés, G. Matz, and F. Hlawatsch, "Linear time-varying channels," Inst. Commun. Radio-Frequency Eng., Vienna Univ. Technol., Tech. Rep. #98-06, Dec. 1998.

[39] I. S. Reed, "On a moment theorem for complex Gaussian processes," *IEEE Trans. Inform. Theory*, vol. IT-8, pp. 194–195, June 1962.

[40] L. Isserlis, "On a formula for the product-moment coefficient in any number of variables," *Biometrika*, vol. 12, pp. 134–139, 1918.

Harold Artés (S'98) received the Dipl.-Ing. degree in electrical engineering from Vienna University of Technology, Vienna, Austria, in 1997.

Since then, he has been a Research (and partly Teaching) Assistant with the Institute of Communications and Radio-Frequency Engineering, Vienna University of Technology, where he is currently working toward the Ph.D. degree. His research interests include MIMO wireless communications, blind estimation and equalization of time-varying channels, and multiuser techniques.

Mr. Artés participated in the European Union funded IST project ANTIUM and co-authored two patents.

Gerald Matz (M'01) received the Dipl.-Ing. and Dr. techn. degrees in electrical engineering from Vienna University of Technology, Vienna, Austria, in 1994 and 2000, respectively.

Since 1995, he has been with the Institute of Communications and Radio-Frequency Engineering, Vienna University of Technology. His research interests are in the areas of wireless communications, statistical signal processing, and time-frequency methods.

Franz Hlawatsch (SM'00) received the Dipl.-Ing., Dr. techn., and habilitation degrees in electrical engineering/signal processing from Vienna University of Technology, Vienna, Austria, in 1983, 1988, and 1996, respectively.

Since 1983, he has been with the Institute of Communications and Radio-Frequency Engineering, Vienna University of Technology, where he currently holds an Associate Professor position. He worked as a consultant for Schrack AG from 1983 to 1988 and for AKG GesmbH from 1984 to 1985. From 1991 to 1992, he spent a sabbatical year with the Department of Electrical Engineering, University of Rhode Island, Kingston. In 1999, 2000, and 2001, he held one-month Visiting Professor positions at ENSEEIHT, Toulouse, France, and IRCCyN, Nantes, France. He is the author or co-author of two books and over 130 scientific papers and book chapters, co-editor of two books, and co-author of two patents. His research interests are in nonstationary statistical and time-frequency signal processing and wireless communications.

Dr. Hlawatsch participated in the European Union funded IST project ANTIUM and directed six research grants given by the Fonds zur Förderung der wissenschaftlichen Forschung (the Austrian science funding organization). He is currently serving as an Associate Editor of the IEEE TRANSACTIONS ON SIGNAL PROCESSING.